

CAPS Simulation Environment Development⁸

DOUGLAS G. MURPHY

Analytical Mechanics Associates, Inc.

JAMES A. HOFFMAN

Analytical Mechanics Associates, Inc.

Introduction

The final design for an effective Comet/Asteroid Protection System (CAPS) will likely come after a number of competing designs have been simulated and evaluated. Because of the large number of design parameters involved in a system capable of detecting an object, accurately determining its orbit, and diverting the impact threat, a comprehensive simulation environment will be an extremely valuable tool for the CAPS designers. A successful simulation/design tool will aid the user in identifying the critical parameters in the system and eventually allow for automatic optimization of the design once the relationships of the key parameters are understood.

A CAPS configuration will consist of space-based detectors whose purpose is to scan the celestial sphere in search of objects likely to make a close approach to Earth and to determine with the greatest possible accuracy the orbits of those objects. Other components of a CAPS configuration may include systems for modifying the orbits of approaching objects, either for the purpose of preventing a collision or for positioning the object into an orbit where it can be studied or used as a mineral resource. The Synergistic Engineering Environment (SEE) is a space-systems design, evaluation, and visualization software tool being leveraged to simulate these aspects of the CAPS study. The long-term goal of the SEE is to provide capabilities to allow the user to build and compare various CAPS designs by running end-to-end simulations that encompass the scanning phase, the orbit determination phase, and the orbit modification phase of a given scenario.

Herein, a brief description of the expected simulation phases is provided, the current status and available features of the SEE software system is reported, and examples are shown of how the system is used to build and evaluate a CAPS detection design. Conclusions and the roadmap for future development of the SEE are also presented.

Comet/Asteroid Protection System Simulations

The scanning phase of the Comet/Asteroid Protection System (CAPS) activity is referred to in the Synergistic Engineering Environment (SEE) as the “Survey Mode” simulation. In this mode a configuration of space-based detectors is scanning the celestial sphere, identifying and cataloguing potentially hazardous objects, and performing preliminary orbit determination. The object of the survey simulation is to evaluate the effectiveness of a given telescope configuration and scanning pattern in identifying potentially hazardous near-Earth objects (NEOs).

The process of evaluating the ability of the CAPS system to properly identify the orbit of an object on a collision course with Earth is referred to as the “precision orbit determination” (POD) simulation. In this mode, one or more simulated NEOs will be placed on a collision course with Earth. The results of these simulations will show how well these orbits were able to be determined at a selected time prior to impact,

⁸Chapter nomenclature available in chapter notes, p. 217.

or the results will return a warning time that indicates how many days prior to impact the system was able to determine that the object was on a collision course.

The process of using the CAPS configuration to evaluate the composition of a given NEO is referred to as the “physical characteristics” simulation. In this mode the simulation will determine the ability of the system to report what the object is made of in order to determine its value as a resource.

Modeling the procedures for averting an impact is referred to as the “orbit modification” simulation. The orbit modification procedures can be divided into two types: deflection mode and resource utilization mode. In both cases the simulation will determine the ability of a given CAPS configuration to make desired orbital adjustments to an approaching object. A deflection case will model the modification of an NEO orbit from an Earth-impacting trajectory to a nonimpacting trajectory. The resource utilization case is not restricted to impacting NEOs and will have additional constraints on the target orbit (e.g., that the new orbit must leave the object more easily accessible for rendezvous missions).

The near-term goals of the SEE CAPS module were to support survey and impact simulations and schedule the physical characteristics and orbit modification simulations for longer term development.

Software Architecture and Current Feature Set

The SEE is a cross-platform application that may be run on Windows, IRIX, and Linux operating systems. The main feature of the SEE is the ability to create and view objects in orbit or on the surface of planets and moons in the solar system. The user interface is designed to allow ease of navigation to points and times of interest in the three-dimensional (3-D) scene. All models including both planets and spacecraft are rendered by default at their actual scales. An interactive scaling command allows the user to create views in which all objects in the scene are to be visible regardless of size.

Running a simulation generally involves creating SEE objects to represent all of the real objects being simulated (e.g., planets, moons, telescopes) and then populating the SEE objects with appropriate parameters (e.g., orbital parameters, detector performance models). An SEE object refers to an entity in the simulation that has properties that can be updated as the simulation progresses. The simulation time is controlled by an event loop, which will cause each of the SEE objects to update its time dependent parameters whenever the current simulation time is changed. The output of the simulation can be in the form of an interactive graphics window that shows the geometry of the scene for a given simulation time, or in data plots, data files, and reports describing the outcome of the run. Figure 1 shows a control flow diagram of an impact analysis loop connected to the main application.

In the current revision of the SEE application, the user must launch the program in an interactive mode; that is, launching the application brings up an application window with graphical user interface (GUI) components. The user must create the simulation objects by adding various craft and minor planets or other natural objects using the GUI or by loading previously saved versions of these objects from files. Once created, the interactive mode will allow the user to vary the current simulation time using a graphical time controller. Once launched, however, the SEE will also support noninteractive analysis by allowing the user to select from a list of data-generating routines such as a survey analysis. An analysis wizard will guide the user through the process of inputting parameters required to run a given analysis, always including a start time, stop time, and time step at which to record data. When the user accepts the analysis parameters and closes the wizard, the event loop is controlled automatically for the duration of the analysis. The event loop controller is responsible for changing the simulation time to the

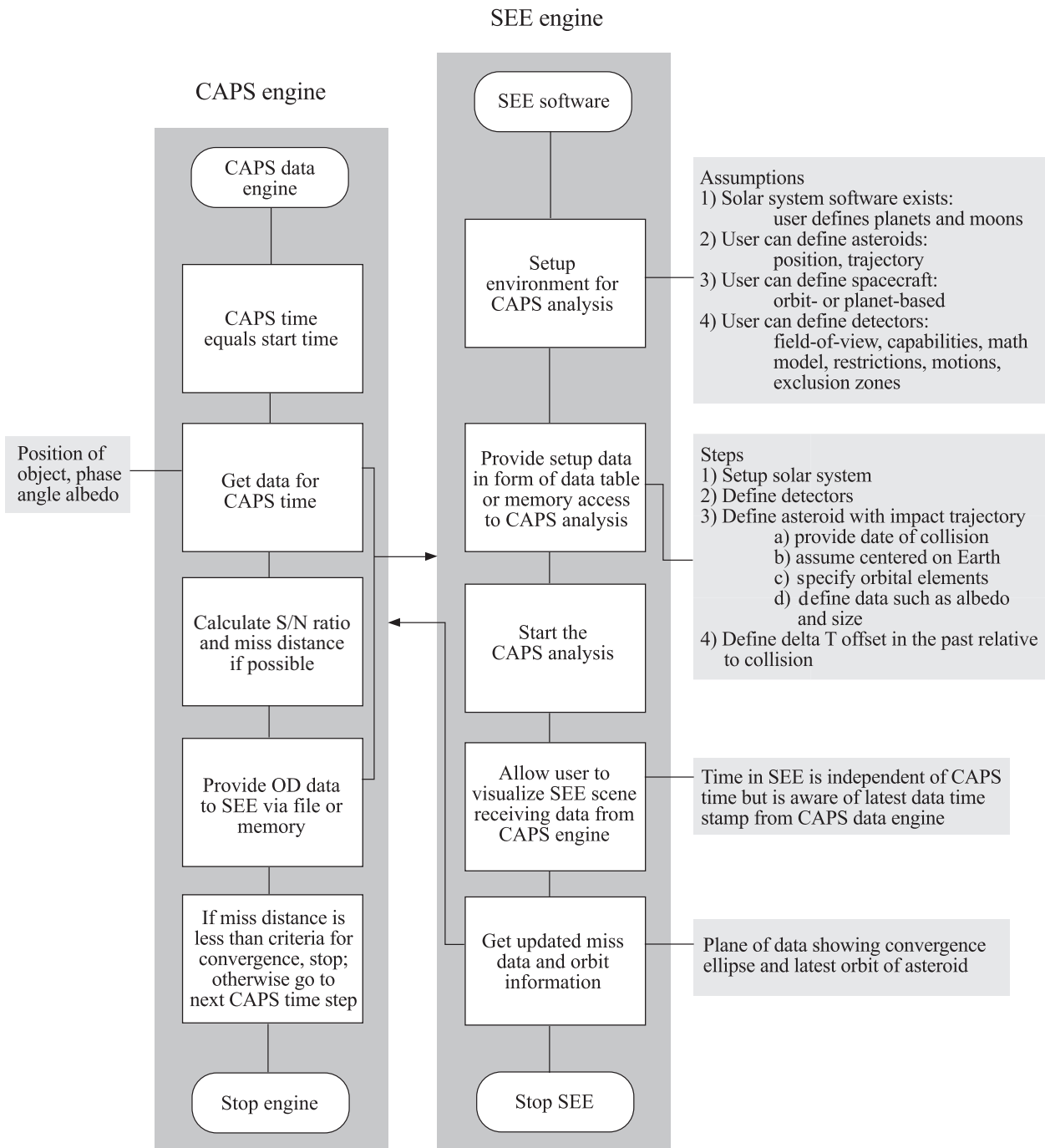


Figure 1. SEE CAPS module control flow.

analysis start time. The controller then polls the SEE objects for data needed for the analysis, processes and saves the data, and advances the simulation time by one analysis time step. The process completes when the analysis stop time is reached. Data files and summary reports containing the results of the simulation can be viewed once the analysis is completed. All interactive navigation controls (except for the time controls) and scaling controls are active and available to the user while the analysis is underway.

The currently implemented features of the SEE support the survey mode simulation and can also be used in the preparation of POD simulations. The survey mode simulation utilizes a helper application called the CAPS Coverage/Sensitivity Tool. A brief review of those capabilities is described subsequently.

SEE and The Coverage/Sensitivity Tool Survey Mode Capabilities

The SEE survey tools comprise features within the main SEE application and a separate coverage visualization application called the CAPS Coverage/Sensitivity Tool. The Coverage/Sensitivity Tool is used to gain insight into the success of a survey pattern with respect to total coverage and measured signal-to-noise (S/N) ratios for approaching objects at a uniform target distance without modeling the flight paths of those objects. The SEE application can then be used to evaluate the survey program against an asteroid/comet data set in which the motion of both the NEOs and the telescopes is modeled. A future goal of this project is to merge the features of the CAPS Coverage/Sensitivity Tool directly into the SEE main execution environment.

The CAPS Coverage/Sensitivity Tool

Overview. Placement of the CAPS survey telescopes will be influenced by the need to efficiently survey the celestial sphere at the desired target radius and the need to maximize the S/N ratio for the observed objects. In this section, a description is given of the CAPS Coverage/Sensitivity Tool and the simplified coverage/sensitivity analyses that have been performed to test the software and begin to understand the system tradeoffs regarding placement of CAPS detection assets. The input to the CAPS Coverage/Sensitivity Tool is a schedule of telescope positions and bore sight direction vectors. The output of the tool is an interactive 3-D visualization of the coverage and sensitivity results. This tool facilitates a trade-off study among architectures and scanning strategies. The time dependent 3-D animations in the CAPS analysis module are useful for refining scanning strategies.

For this analysis the position and bore sight data for the scanning telescopes were generated using the commercially available Satellite Tool Kit (STK) space system modeling software. The format of the position and bore sight data are straightforward ASCII file listing times, positions, and direction vectors for each scope. This file can also be generated using standard spreadsheet software or other tools capable of saving the data in ASCII format. STK was used here instead of the SEE because this analysis took place prior to completion of the SEE software. Once the schedule file is generated, the user may import these data, specify the telescope design parameters, and run the analysis (figs. 2 and 3). After the analysis is run, the user may adjust various rendering properties (fig. 4). The user can display the data as a time dependent animation or control the time manually. The mouse can be used to control the vantage point of the data visualization.

Coverage analysis approach. Coverage analysis is accomplished by choosing a radius, such as 7 astronomical units (au), and examining how well a scanning strategy covers the heliocentric sphere of that radius. In the analysis, one measures where and how often the viewing frusta of the scanning telescopes intersect a given heliocentric sphere. To accomplish this, the sphere is “pixelized” using the algorithm in reference 1. Each pixel represents an approximately equal area region of the sphere (fig. 5).

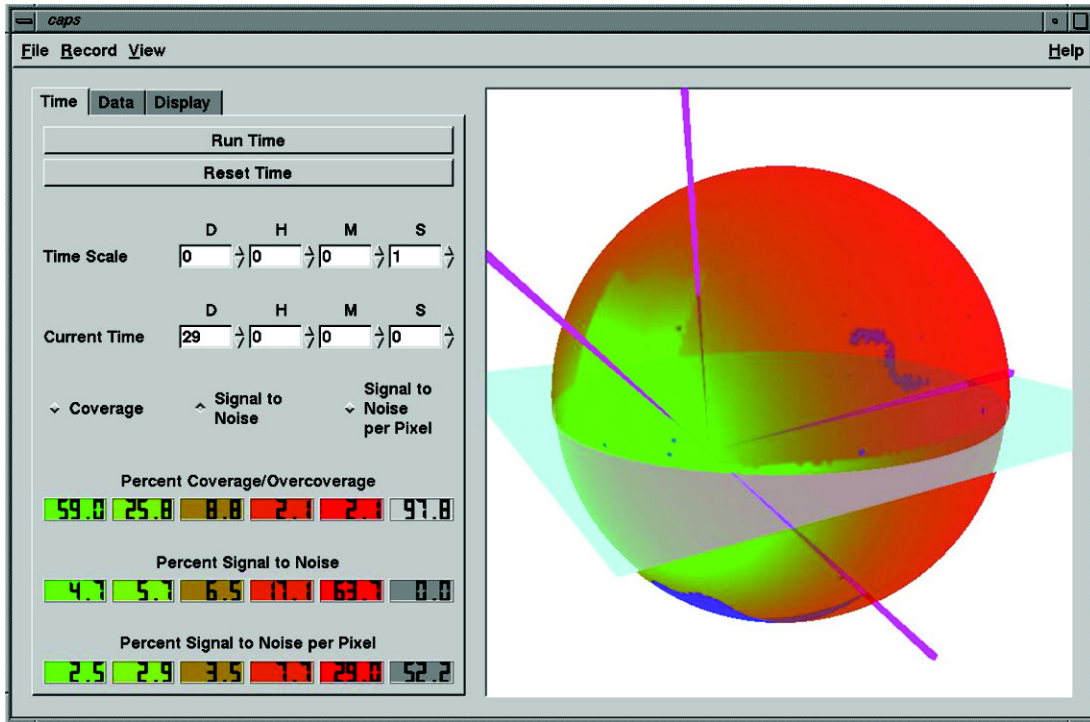


Figure 2. CAPS coverage/sensitivity tool, time inputs.

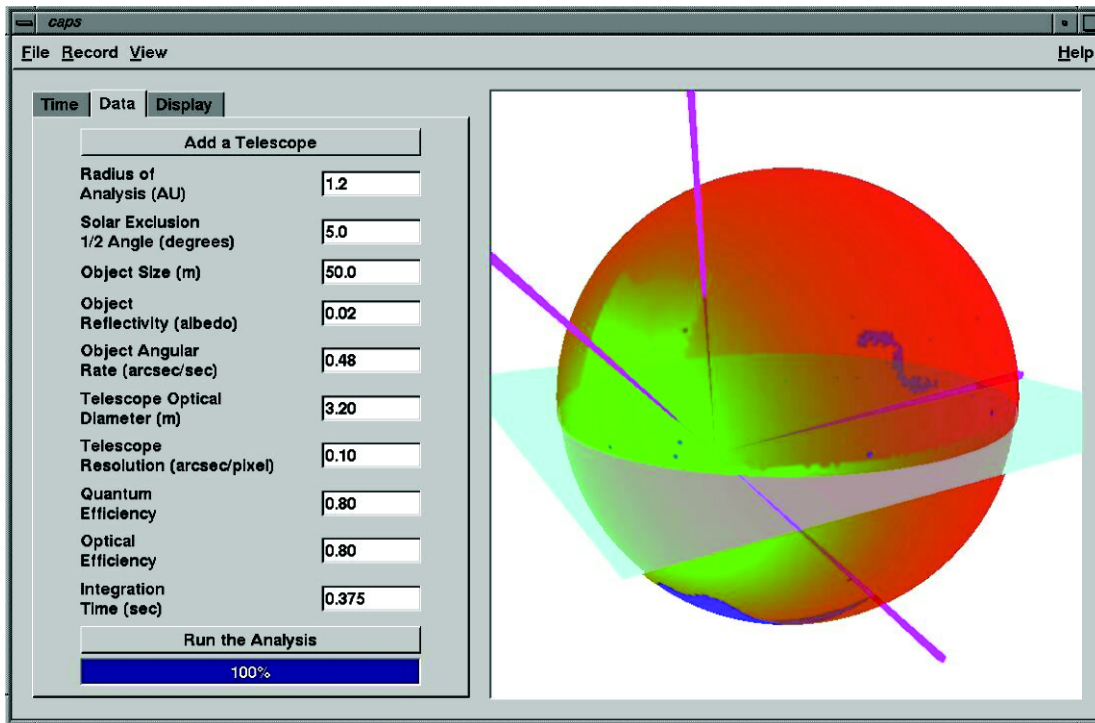


Figure 3. Telescope and NEO data input.

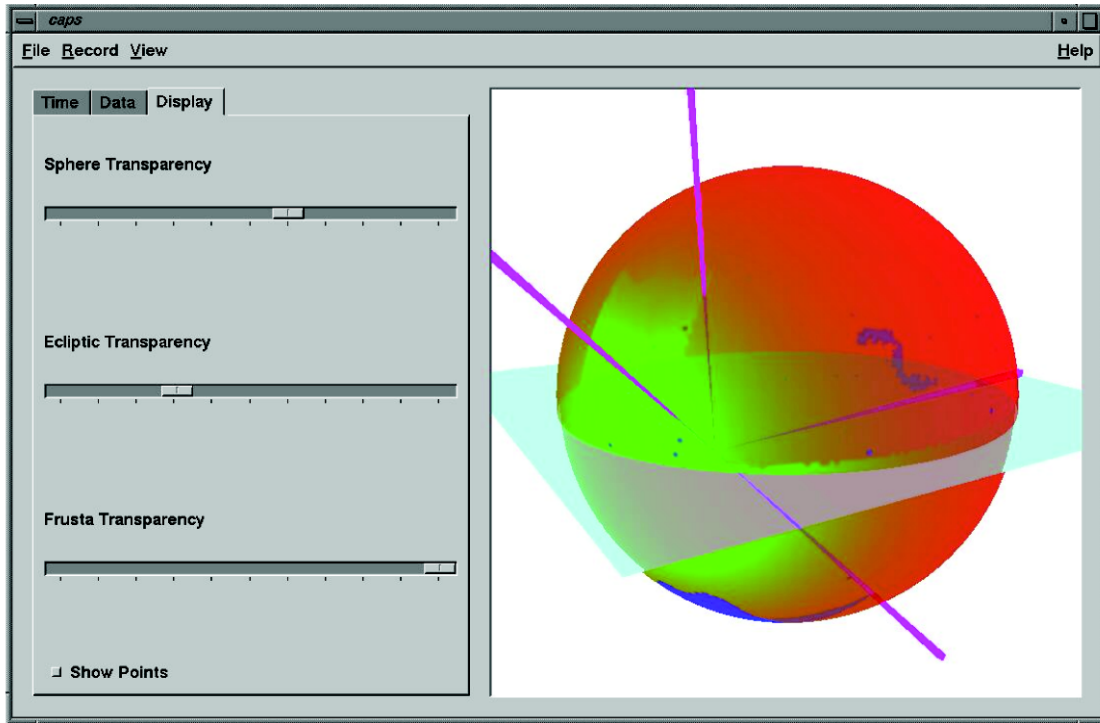


Figure 4. Rendering options.

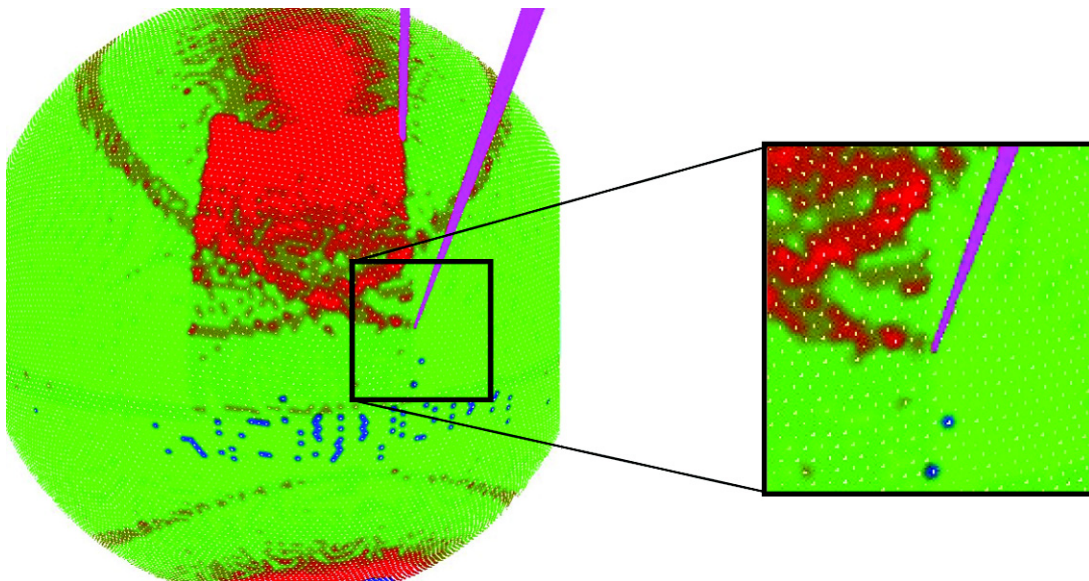


Figure 5. "Pixelizing" the celestial sphere.

The area surrounding a pixel is colored according to how often that pixel is viewed by the scanning telescopes. Initially, each pixel is colored blue to represent an unscanned pixel. A scanned pixel is colored from green to red, a green pixel having been scanned precisely once and a red repeatedly scanned five or more times. In this way, one can differentiate which portions of the sphere are scanned or over-scanned. For example, in figure 5 one sees the reddish-green bands where the polar and equatorial scopes overlap in their scans. One might also note that there is a scattering of unscanned (blue) pixels. This is due to the fact that the displayed scanning strategy allowed for absolutely no overlap in frames. Precision errors likely caused these pixels to lie just outside the scanning pattern of the frustum.

The STK toolkit was used to produce 29 days of position and bore sight data for four lunar-based telescopes. Figure 6 shows a 1.2-au heliocentric sphere (semitransparent) and the viewing frusta of the four telescopes as seen from slightly above the ecliptic plane (in light blue). Figure 7 gives a zenith view and figure 8 gives a view from near Earth (slightly above the ecliptic).

Coverage analysis results. For long-period comets (LPCs), coverage for the four-telescope, lunar-based architecture was tested on a 7-au heliocentric sphere with a 90° solar exclusion half-angle. The analysis was repeated with a 5° solar exclusion half-angle so that one may consider the scanning strategy under the assumption that some idea or device may eventually allow for such an improvement.

For near-Earth asteroids (NEAs), coverage was tested on heliocentric spheres of radii 2, 1.2, and 0.8 au with a solar exclusion half-angle of 45° . Once again, the analysis was repeated with a 5° solar exclusion half-angle. Of particular interest in these cases are the near-Earth views as they describe coverage for objects that are 1 or 0.2 au from Earth.

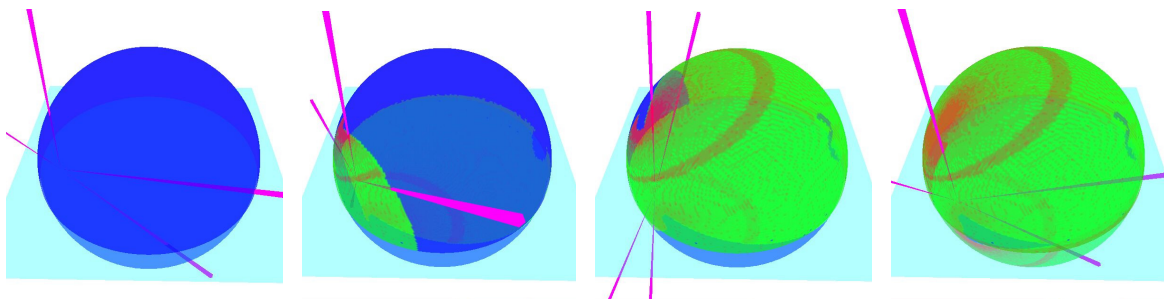


Figure 6. Telescope placement relative to a 1.2-au heliocentric sphere.

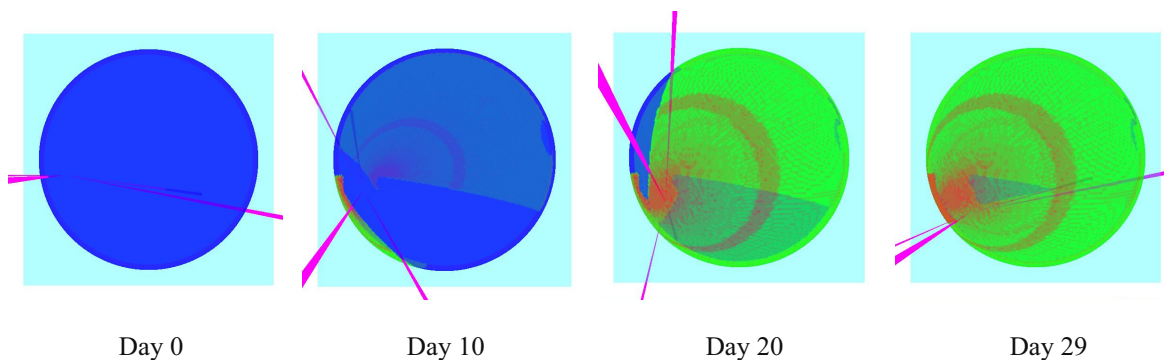


Figure 7. Zenith view of a 1.2-au heliocentric sphere.

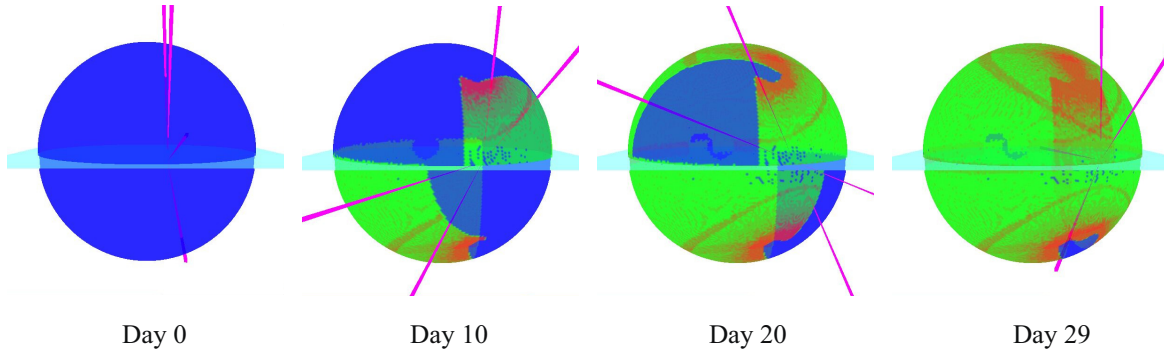


Figure 8. Near-Earth view of a 1.2-au heliocentric sphere.

Tables 1 and 2 give the percentage of the sphere covered by the scanning strategy. It also indicates what percentage of the sphere received single or multiple coverage. It is clear from the percent coverage shown in the tables that solar exclusion is the primary factor for a lunar-based architecture. If one is to achieve a nearly complete scan in 30 days, then either the solar exclusion angle must be reduced or more telescopes are needed in some heliocentric orbit. The multiple coverage in this simple scanning strategy is surprisingly low. One would expect some double coverage if frames are to overlap by a few pixels. Employing a more sophisticated scanning algorithm can reduce the triple (and greater) coverage. One also expects to see some overcoverage on a lunar-based architecture as lunar months overlap, as they do in a 29-day scan.

Table 1. Coverage Analysis With a 90° (7 au only) or 45° Solar Exclusion Half-Angle

| Radius of sphere, au | Coverage, percent | Single coverage, percent | Double coverage, percent | Triple coverage, percent | Quadruple coverage, percent | Over-coverage (5 or more), percent |
|----------------------|-------------------|--------------------------|--------------------------|--------------------------|-----------------------------|------------------------------------|
| 7 | 43.2 | 24.2 | 11.8 | 4.2 | 1.4 | 1.6 |
| 2 | 72.4 | 37.8 | 21.1 | 8.2 | 2.5 | 2.8 |
| 1.2 | 58.8 | 29.8 | 17.5 | 7.4 | 2.0 | 2.1 |
| 0.8 | 33.6 | 18.3 | 10.6 | 3.6 | 1.0 | 0.1 |

Table 2. Coverage Analysis With a 5° Solar Exclusion Half-Angle

| Radius of sphere, au | Coverage, percent | Single coverage, percent | Double coverage, percent | Triple coverage, percent | Quadruple coverage, percent | Over-coverage (5 or more), percent |
|----------------------|-------------------|--------------------------|--------------------------|--------------------------|-----------------------------|------------------------------------|
| 7 | 99.8 | 56.2 | 27.7 | 9.6 | 3.0 | 3.3 |
| 2 | 99.2 | 57.5 | 26.9 | 9.4 | 2.6 | 2.9 |
| 1.2 | 97.8 | 59.0 | 25.8 | 8.8 | 2.1 | 2.1 |
| 0.8 | 95.0 | 64.4 | 23.8 | 5.4 | 1.2 | 0.1 |

Figures 9 through 12 give the visual representation of this analysis. Screen shots were taken from zenith, nadir, near-Earth, and the opposing far side (see figs. 7 and 8). The reddish-green bands in each of these images identify the overlap between two scanning telescopes. The reddish-green sector in the near-Earth (upper hemisphere) and far side (lower hemisphere) identify the overlap is scanning due to lunar orbit. Also, note the gap in coverage seen in the nadir views of the 1.2 and 0.8 au spheres that is also attributable to the lunar orbit. Either a modification in the scanning strategy is needed or one must accept a scanning period of greater than 29 days.

Sensitivity analysis approach. A sensitivity analysis is performed in a fashion similar to the coverage analysis described previously. First, a heliocentric sphere is chosen and pixelized. For each pixel scanned by a telescope, the signal-to-noise (S/N) ratio is computed based on a user input set of telescope parameters. Analysis of the survey telescope design with blur centroiding incorporated demonstrated that the S/N ratio for each scan can be reduced to 3.6 and still provide positive indication of a target. The area representing that pixel is then colored according to the value of the S/N ratio. Values of 1 or less are colored gray with lighter shades close to 1 and darker shades close to 0. Ratios greater than 1 and less than 3.6 are colored on a continuous scale between red and green. Values near 1 are colored red and values near 3.6 are green. Ratios greater than 3.6 are also colored green. If a pixel is scanned multiple times, then the largest S/N ratio found for that pixel is used.

Sensitivity analysis results. For all cases, the telescope was assumed to have an optical diameter of 3.2 m with quantum and optical efficiencies of 0.8. The integration time for the LPC is assumed to be 15 s. An integration time of 0.375 s is assumed for NEAs.

Tables 3 and 4 give the percentage of the sphere scanned within a given range of sensitivity, or S/N ratio. The sensitivity for LPCs is well within the tolerance limit of 3.6.

Table 3. Sensitivity Analysis With a 90° (7 au only) or 45° Solar Exclusion Half-Angle

| Radius of sphere, au | S/N > 3.6, percent | 1.0 < S/N < 3.6, percent | S/N ≤ 1.0, percent |
|----------------------|--------------------|--------------------------|--------------------|
| 7 | 43.2 | 0 | 0 |
| 2 | 0 | 7.5 | 64.9 |
| 1.2 | 4.7 | 54 | 0 |
| 0.8 | 3.5 | 30.3 | 0 |

Table 4. Sensitivity Analysis With a 5° Solar Exclusion Half-Angle

| Radius of sphere, au | S/N > 3.6, percent | 1.0 < S/N < 3.6, percent | S/N ≤ 1.0, percent |
|----------------------|--------------------|--------------------------|--------------------|
| 7 | 99.8 | 0 | 0 |
| 2 | 0 | 7.5 | 91.7 |
| 1.2 | 4.7 | 93.1 | 0 |
| 0.8 | 3.8 | 91.1 | 0.1 |

For NEAs, coverage was tested on heliocentric spheres of radii 2, 1.2, and 0.8 au with a solar exclusion half-angle of 45°. The object was assumed to be 50 m in diameter with an albedo of 0.02. As before, the analysis was repeated with a 5° solar exclusion half-angle. A schematic of the orbits assumed for NEA sensitivity analysis is shown in figure 13.

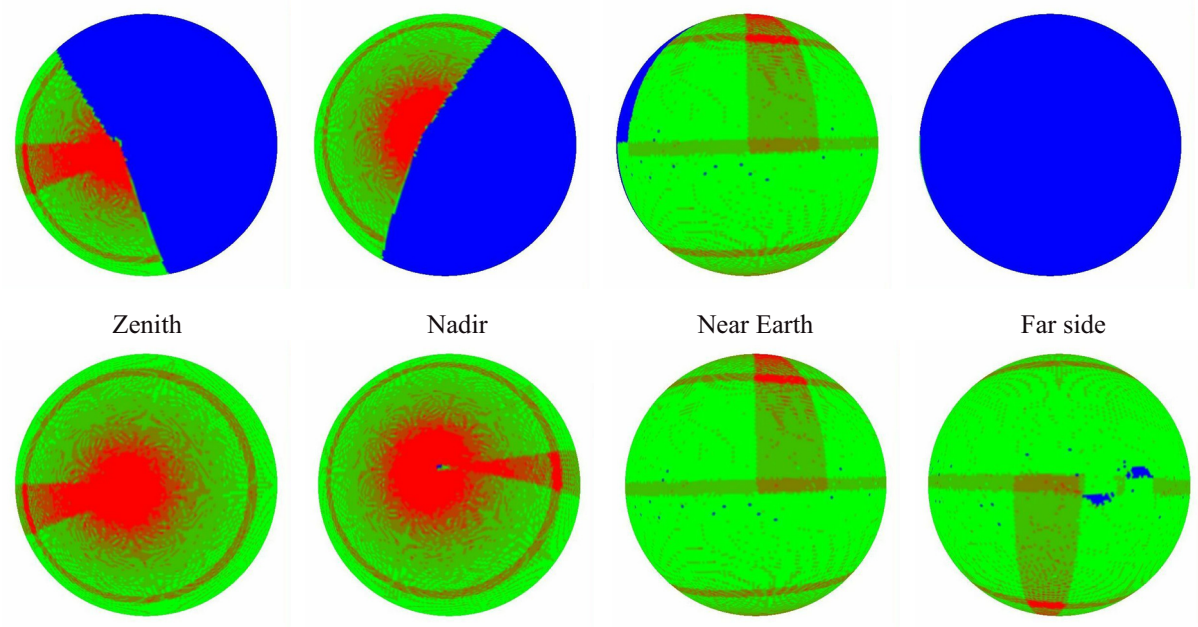


Figure 9. Coverage of a 7-au heliocentric sphere with 90° half-angle (top) and 5° half-angle (bottom).

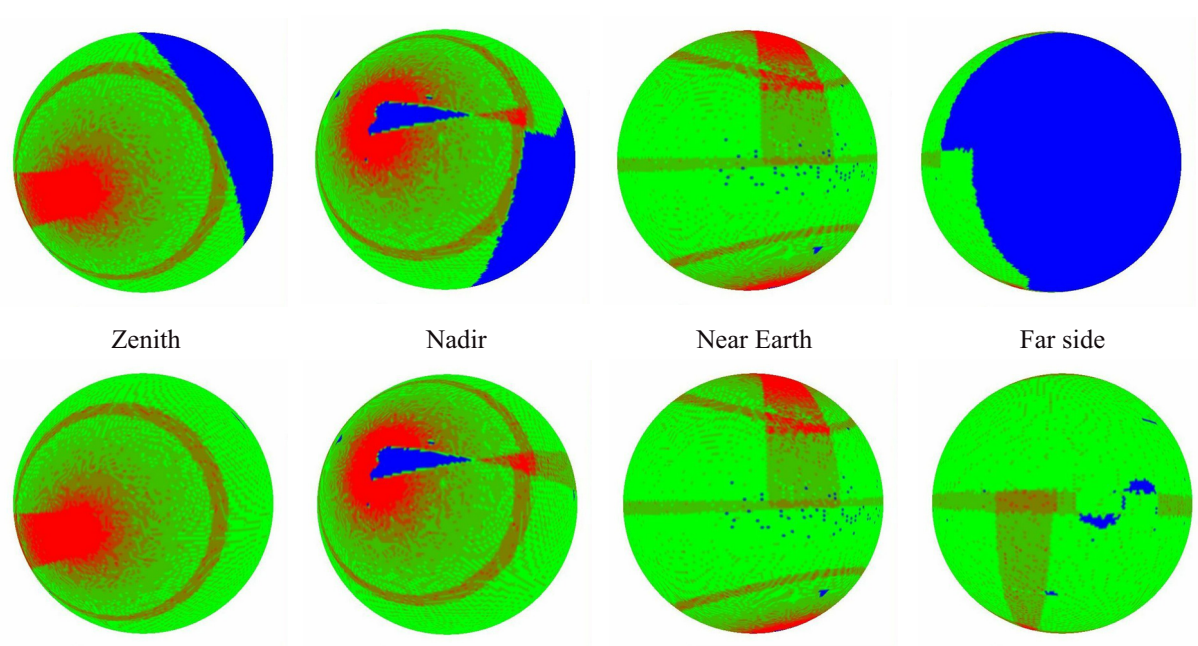


Figure 10. Coverage of a 2-au heliocentric sphere with 45° half-angle (top) and 5° half-angle (bottom).

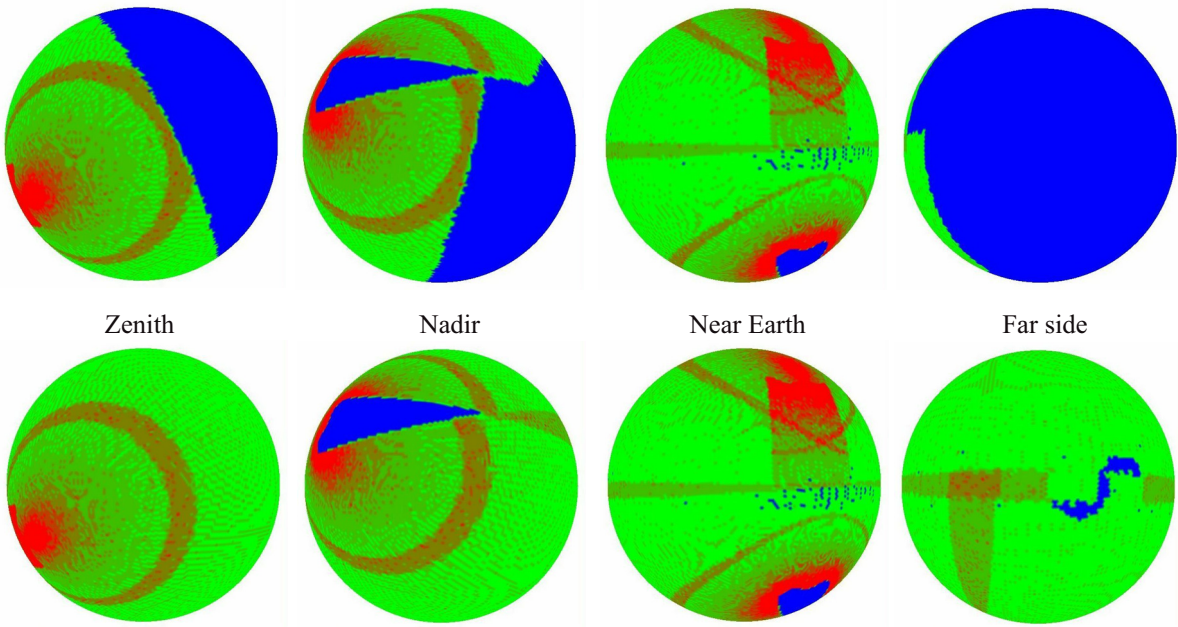


Figure 11. Coverage of a 1.2-au heliocentric sphere with 45° half-angle (top) and 5° half-angle (bottom).

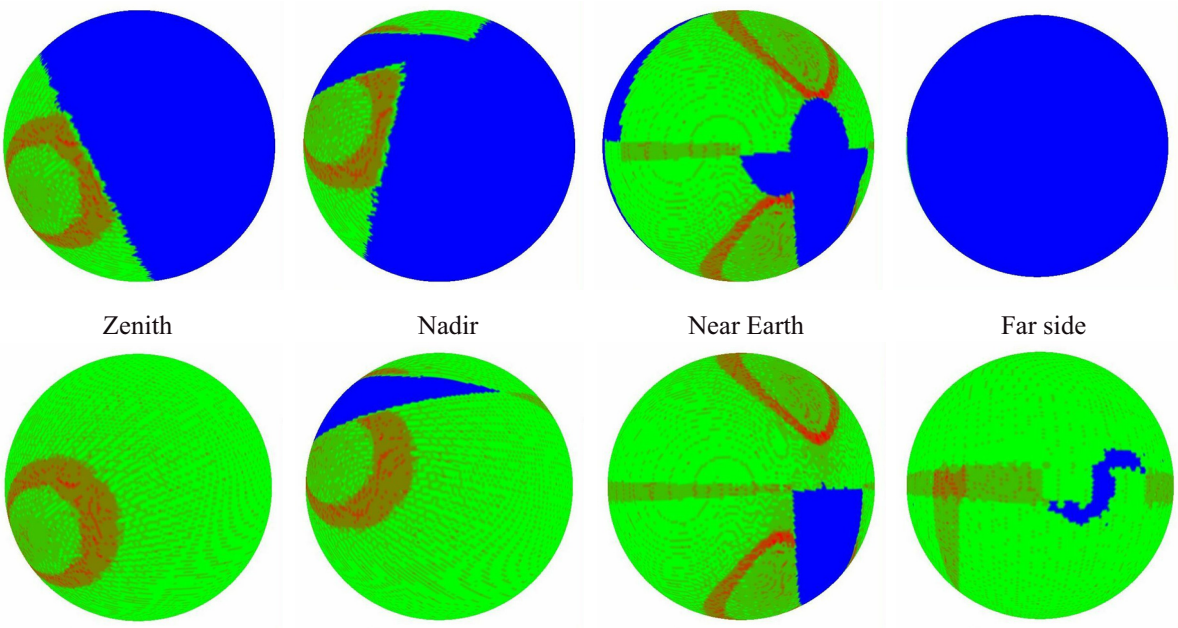


Figure 12. Coverage of a 0.8-au heliocentric sphere with 45° half-angle (top) and 5° half-angle (bottom).

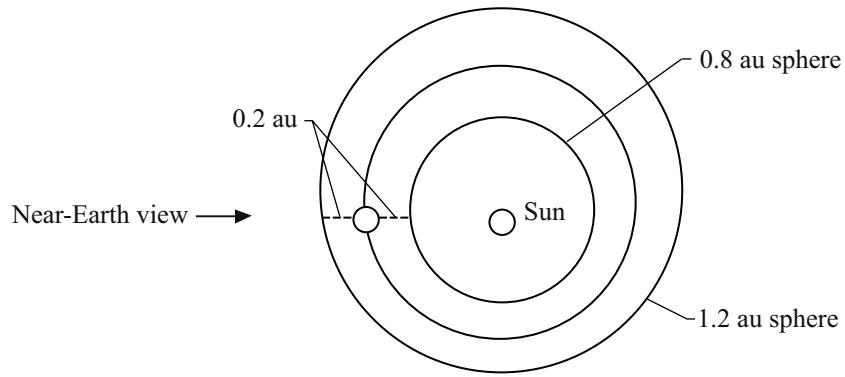


Figure 13. Orbit diagram for near-Earth asteroid sensitivity analysis.

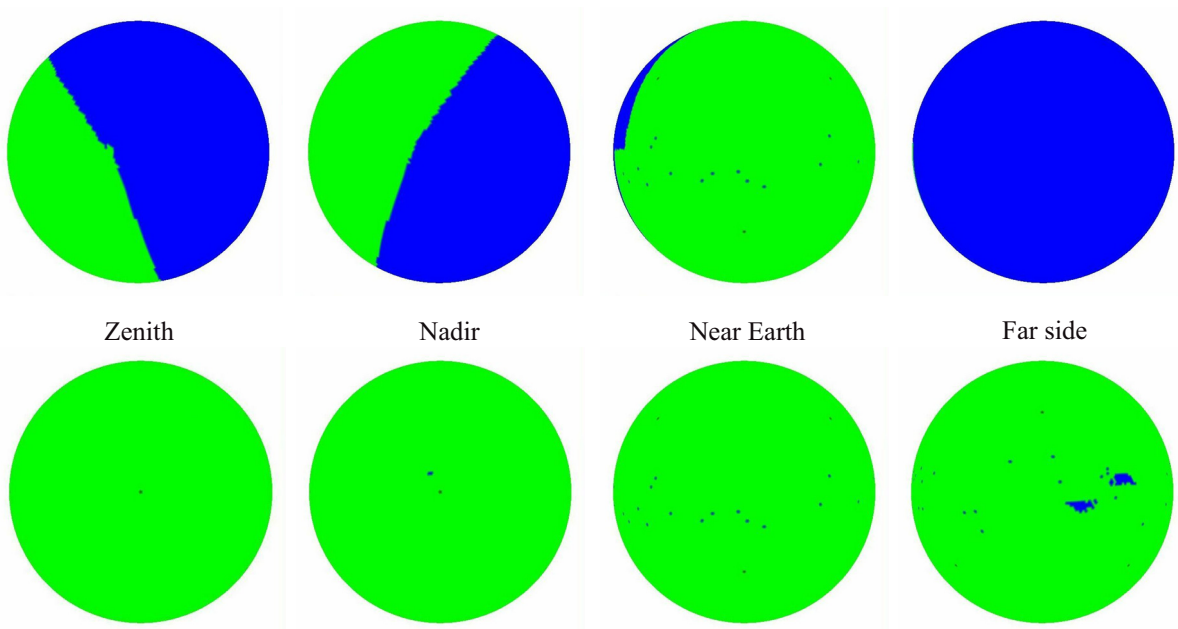


Figure 14. Sensitivity for a 7-au heliocentric sphere with 90° half-angle (top) and 5° half-angle (bottom).

For LPCs, sensitivity for the four-telescope, lunar-based architecture was tested on a 7-au heliocentric sphere with a 90° solar exclusion half-angle. The object was assumed to be 1000 m in diameter with an albedo of 0.02. The analysis was repeated with a 5° solar exclusion half-angle so that one may consider the scanning strategy under the assumption that some idea or device may eventually allow for such an improvement. The results of these simulations are shown in figure 14.

The NEAs within 0.2 au of the Earth are also within this tolerance. This can be noted from the near-Earth views of the 1.2- and 0.8-au heliocentric spheres in figures 15 and 16. The NEAs at 1 au from the Earth are generating S/N ratios close to 1, as can be seen by the bright red splotch on the near-Earth view in figure 17.

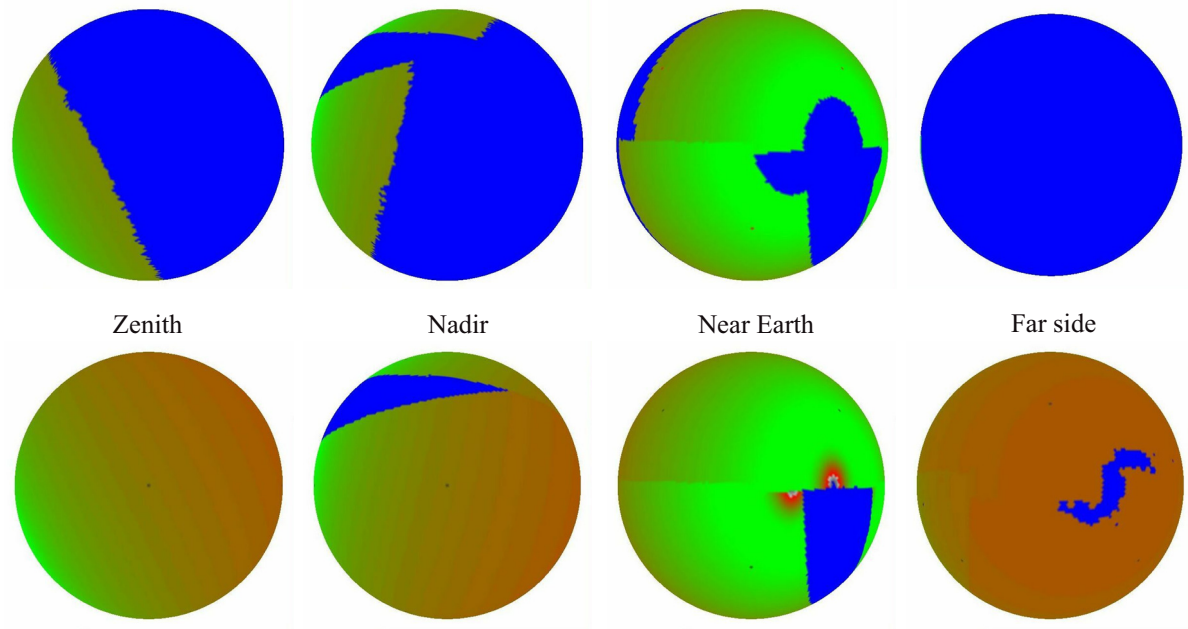


Figure 15. Sensitivity for a 0.8-au heliocentric sphere with 45° half-angle (top) and 5° half-angle (bottom).

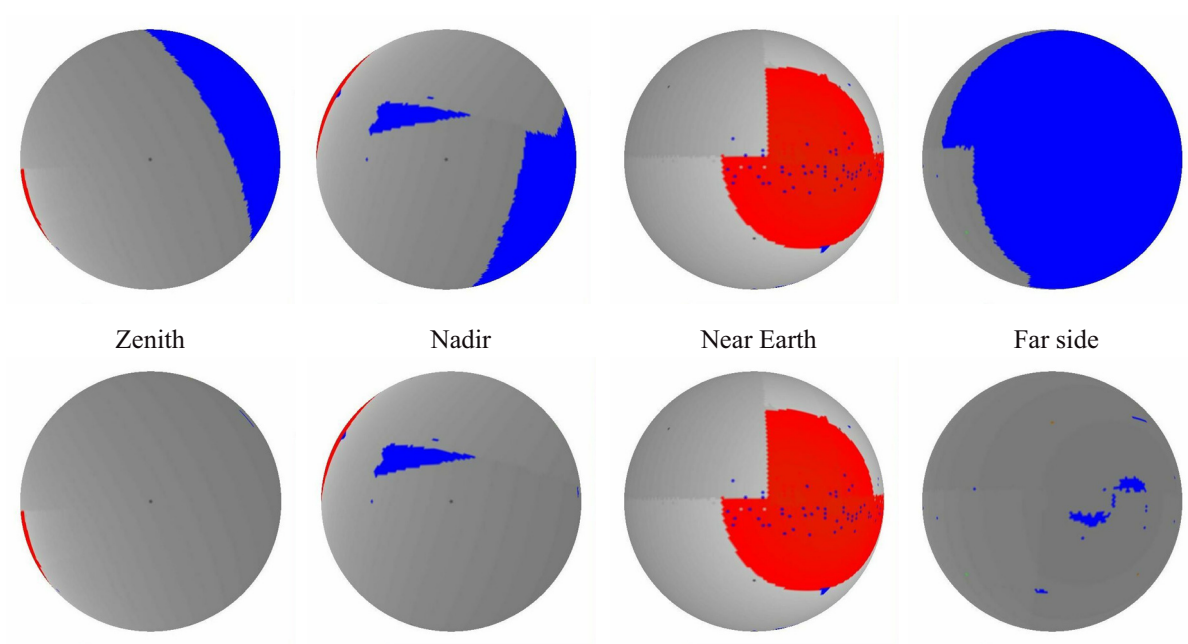


Figure 16. Sensitivity for a 2-au heliocentric sphere with 45° half-angle (top) and 5° half-angle (bottom).

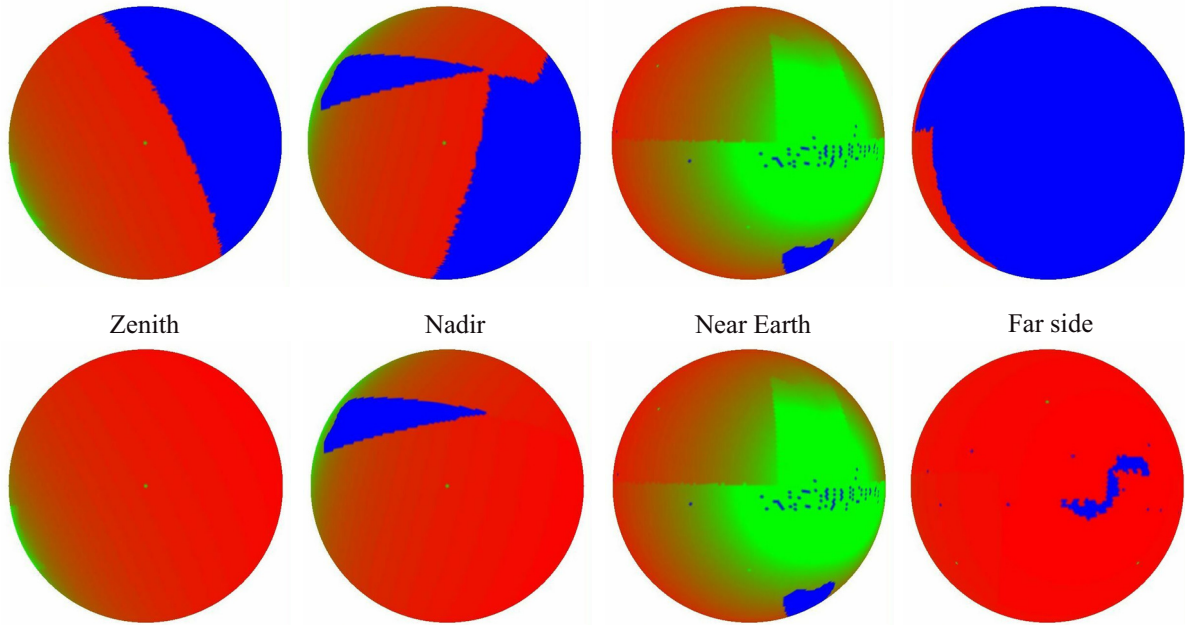


Figure 17. Sensitivity for a 1.2-au heliocentric sphere with 45° half-angle (top) and 5° half-angle (bottom).

The Synergistic Engineering Environment. The limitation of the Coverage/Sensitivity Tool is that the NEO motion cannot be modeled. Also, the position and orientation of the detectors is fixed once the detector schedule is read in. The SEE addresses these issues by allowing the user to import data sets of classical orbital elements to define two-body keplerian orbits for many thousands of objects. The SEE user also has interactive control of the detector placement in orbit or on the surface of a planet or moon.

In figure 18, a screen capture of a survey simulation in progress in the SEE is shown. The current release supports the ability to import up to 25000 minor planets using orbit data read from a text file (the upper limit of the object population may be higher depending on the system hardware). All these objects can be scaled and tethered to for visualization purposes. Figure 19 is a view from the bore sight of one of the detectors, with several NEOs (pyramid shaped objects) in view.

At present, the list of objects to be loaded into the scene is specified at application launch time by selecting an SEE mission from a file browser dialog box. The mission file also specifies the number and type of crafts to be loaded into the scene. The ability to interactively import a single object or a collection of objects into the scene at any time is a planned near-term enhancement. The craft objects can be placed in orbit around or on the surface of any planet in the solar system. Code for interactively modifying the orbits of various craft is in place. The properties of the detectors, physical properties of the NEOs, and the parameters of the scanning algorithm have been hard coded into this version of the application in order to conduct testing. Further enhancements are planned to support the automatic generation of efficient scanning algorithms for a given configuration of detectors and to modify the parameters of the detectors.

A short report that lists by name the NEOs currently in the field-of-view (FOV) of each of the telescopes is available at any time step (fig. 20). Additionally, a complete survey analysis can be launched via the survey simulation wizard. The wizard prompts the user for the survey start time, survey end time, frame integration time, and a radius at which to record the coverage map. Once the parameters are

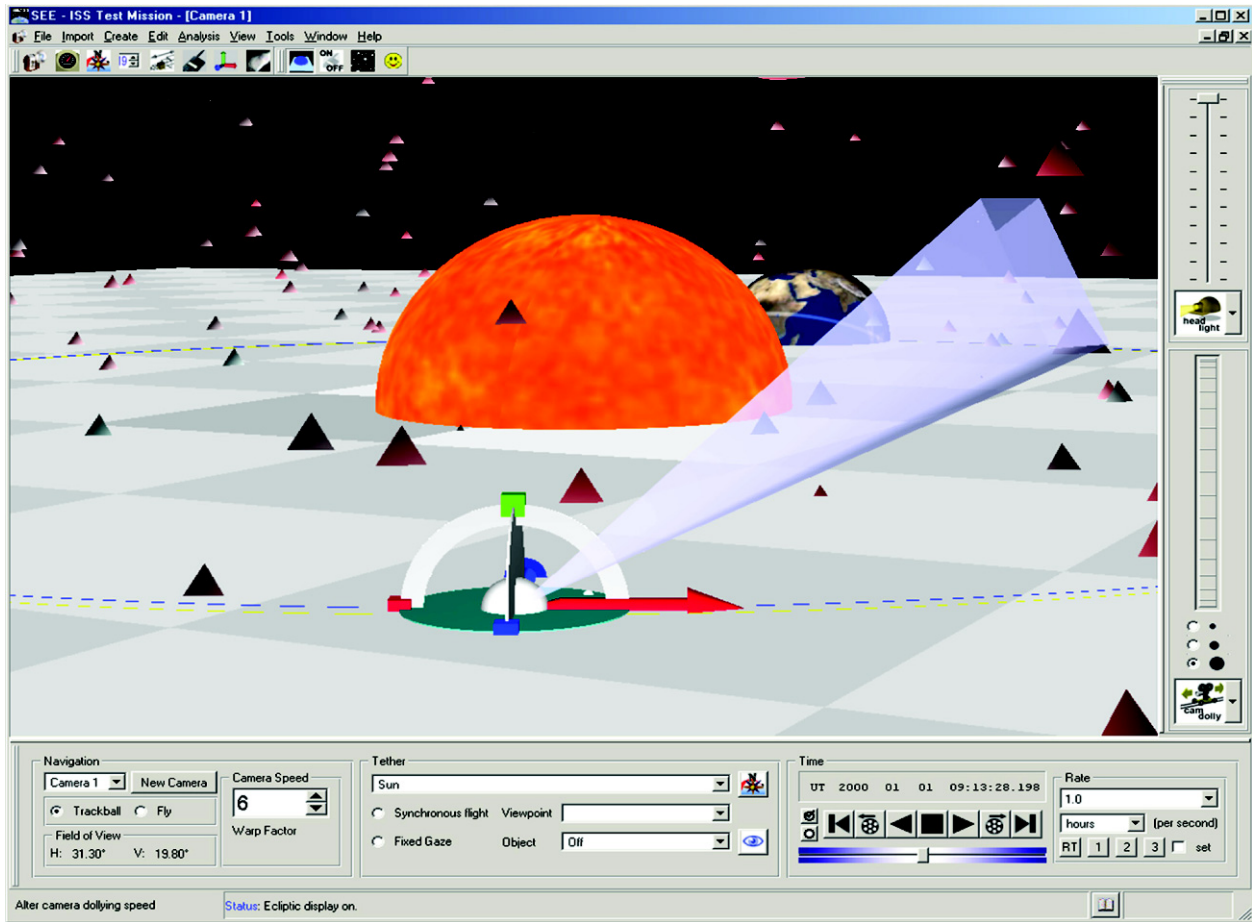


Figure 18. SEE application screen: survey simulation in progress.

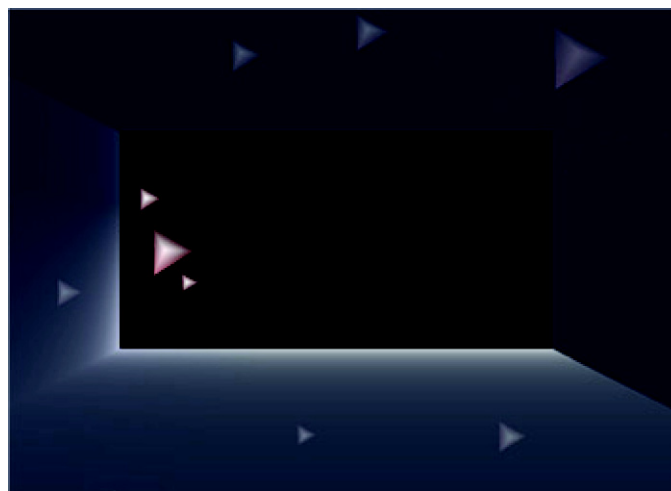


Figure 19. View from detector.

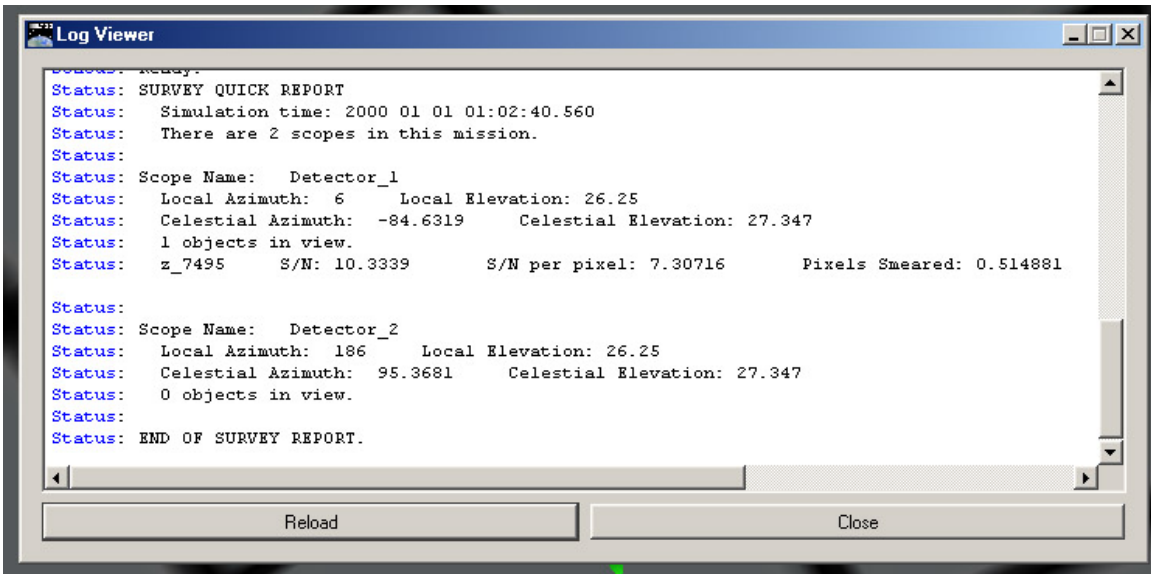
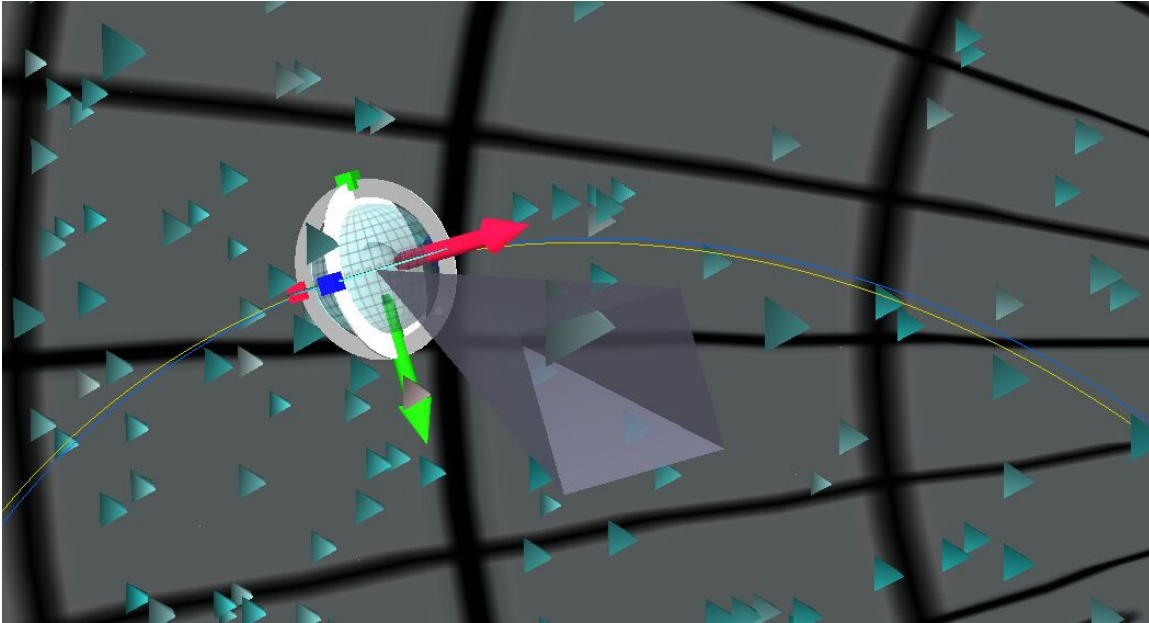


Figure 20. Quick survey report with one NEO in FOV.

accepted, a survey analysis thread is launched, and a progress bar displays the completion percentage. During the full survey analysis an interactive coverage map is displayed (fig. 21). The map depicts areas of the target sphere that have been covered by the detectors in the survey. The dotted grey lines represent lines of latitude and longitude of the target sphere in a sinusoidal projection. The central horizontal line represents the target sphere equator, and the top and bottom points of the projection represent the north and south poles of the target sphere. Blue rectangles with black outlines are drawn in areas of the map corresponding to areas of the target sphere that have been “covered” by the detectors. An area is considered covered if it has been inside the detector view frustum while the detector was collecting data. The map view may be browsed while the analysis is running by using pan and zoom functions in the map window. The native resolution of the bitmap is 3600×1800 pixels.

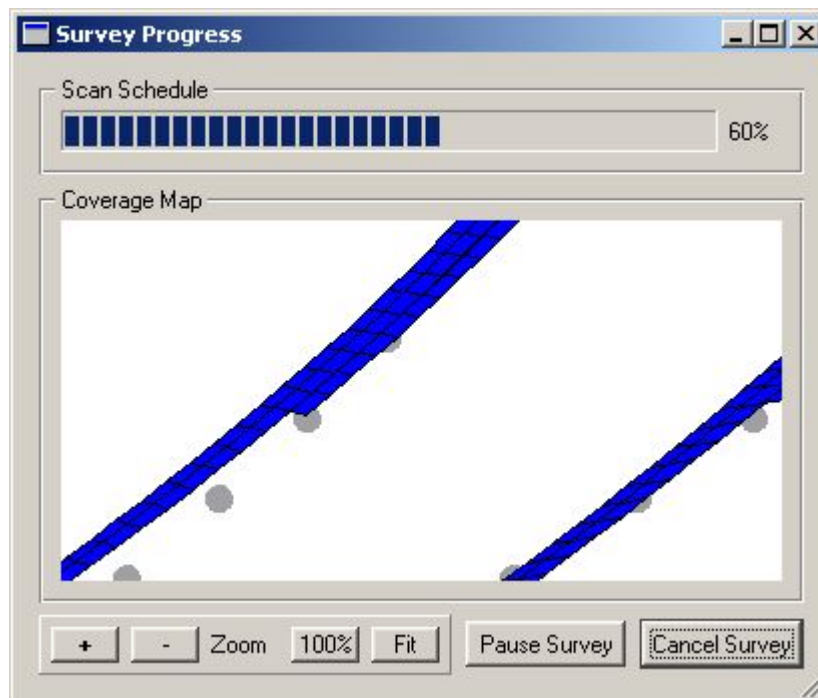
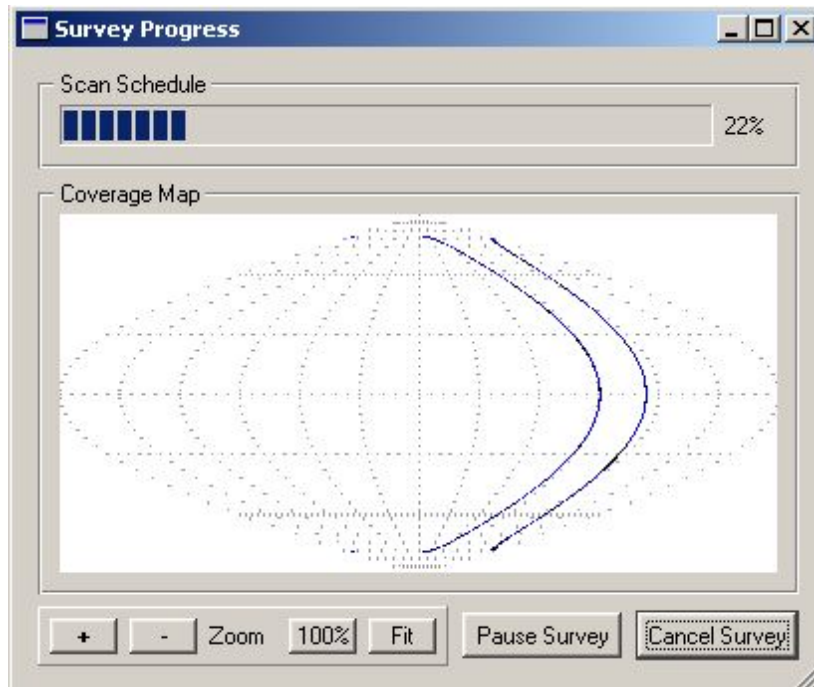


Figure 21. Interactive coverage map.

The purpose of the interactive coverage map is to give the user immediate qualitative feedback on the effectiveness of the proposed scanning strategy. The algorithm for drawing the coverage map employs an intersection technique to find the points at which the corners of the rectangular detector view frustum intersect the target sphere. These points are used to draw a filled blue rectangle with a black outline on the coverage map. This intersection algorithm is computationally efficient and does not noticeably impact the speed of the simulation. However, because the edges of the filled rectangle are straight lines rather than sphere segments, the map is an approximation of the actual coverage. For view-frusta larger than those being considered here, a sphere pixelization technique would provide more accurate results at a much greater computational expense. For efficiency reasons, the overcoverage of the target sphere is not directly measured in this algorithm. However, a qualitative sense of the amount of overcoverage may be gained by examining the density of the black outlines drawn around the blue-filled rectangles (see fig. 22). Areas of substantial overcoverage will have more closely spaced black lines.

The coverage map does not account for data-taking exclusion zones caused by light from the Sun or by physical occlusions of the detector view by planets and moons. The Coverage/Sensitivity Tool can be used to examine these effects if desired.

When the survey is complete a series of reports are written. These include one report file for each detector in the scene and one summary report file. The detector reports contain a review of the detector and survey parameters and a list of observed NEOs at each time step in which at least one NEO was in the telescope FOV. The summary report lists how many NEOs were never detected during the survey and lists those objects by name. These reports include measured S/N and per-pixel S/N values for each observation, as well as survey statistics. Future enhancements include the ability to consider exclusion zones for a detector FOV caused by bright objects such as the Sun or Jupiter, or by physical blockages by objects obstructing the view cone or frustum.

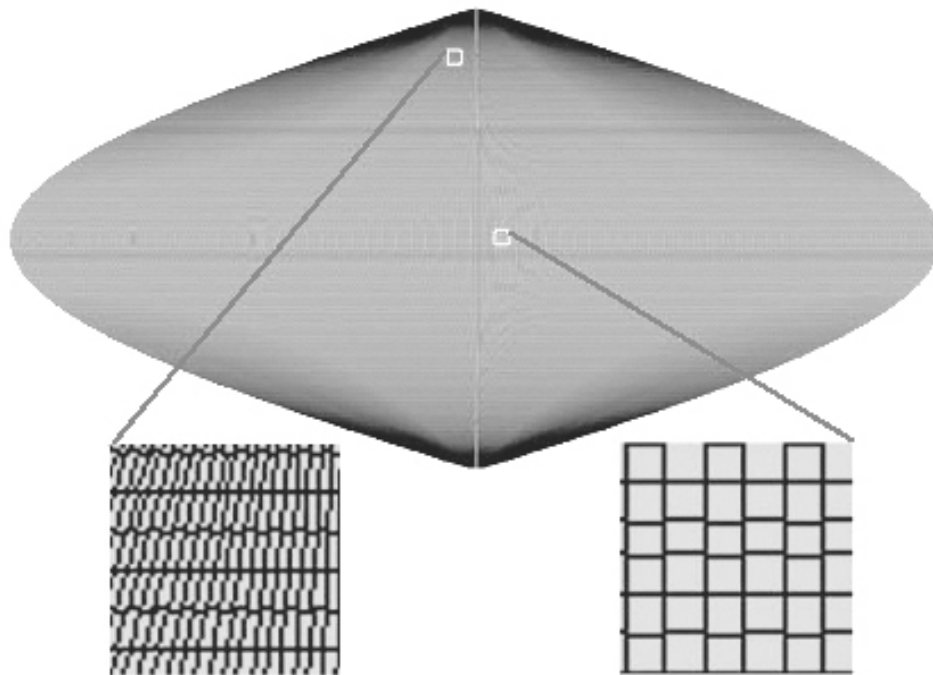


Figure 22. Case 1 target sphere coverage map.

Impact Simulations

To follow is a description of the current and planned capabilities of the SEE that relate to conducting a CAPS impact simulation. A simulated Earth impactor being viewed from two vantage points as part of an impact analysis is shown in figure 23 (note that the impactor scale is greatly exaggerated in the right-hand image). At present, the SEE allows a user to create an impacting asteroid by loading a trajectory file that contains position versus time, or position and velocity versus time data. It is assumed that if the object being imported is identified as an impactor, the trajectory data describe a path that intersects the ecliptic at 1 au. If the Earth is defined as having a zero eccentricity, zero inclination orbit with the semi-major axis at exactly 1 au, algorithms in the SEE will be able to assign an epoch to the NEO trajectory data that will cause an Earth impact in an arbitrary simulation year. If the simulated Earth orbit does not exactly meet the above parameters, the epoch will still be resolved for a closest Earth approach but may not generate an impact.

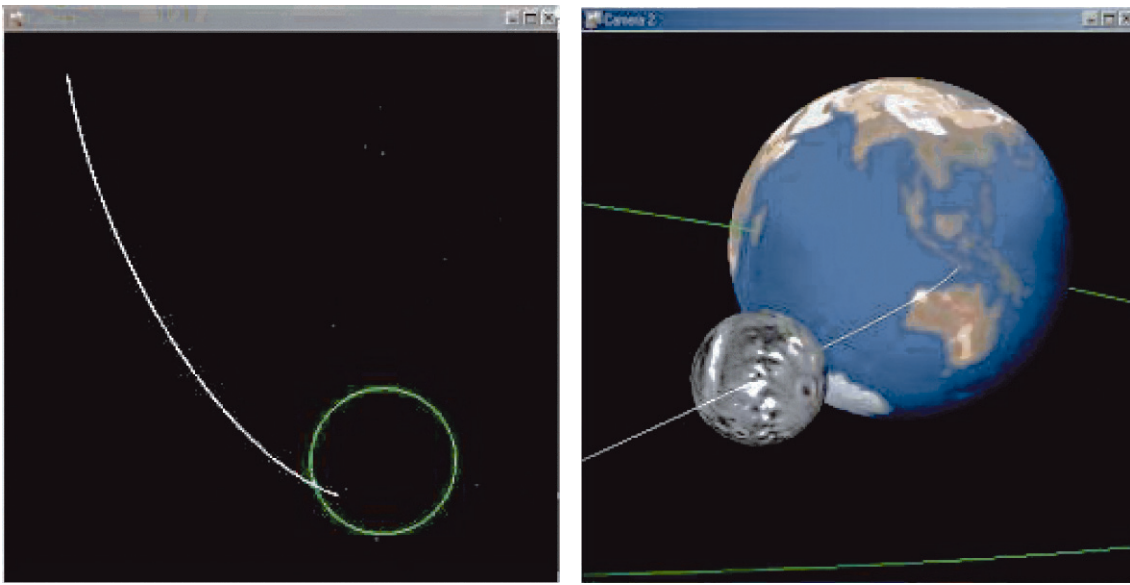


Figure 23. Earth impactor.

Future enhancements are planned that will allow the user to create a minor planet that impacts the Earth or another planet at any selected date, without requiring the user to supply trajectory data.

A POD analysis is conducted in the current version of the SEE by first creating one or more CAPS observatories and then one impacting NEO. Selecting “precision orbit determination” from the analysis pull-down menu will then launch the POD wizard, which guides the user through the process of inputting the required parameters. Among the required parameters is the date of the first observation of an NEO by observatory. If the user prefers to gauge the first observation opportunity in terms of distance to the object from the observatories rather than by selecting a date, a range GUI is provided under the tools pull-down menu. The range GUI displays the current distance between any two objects in the scene. The user may initially adjust the simulation time controls until the range GUI reports the desired distance at which to begin the observations; then the user includes the corresponding date to populate the date field of the POD wizard.

When the POD wizard is completed, a POD analysis thread is launched to collect the data required for the POD report. The POD report contains time stamped data describing the location of the observatories, the direction of the NEO with respect to these observatories, and the position and velocity of the NEO. The POD report file can be read directly into the Matlab®/Simulink® POD system used to generate the reconstructed trajectories and the erroneous predicted miss distance (EPMD). Future enhancements are planned that will allow the reconstructed trajectories and an error ellipsoid (a metric designed to indicate the margins of error associated with the collections of reconstructed trajectories) to be imported into the SEE and visualized.

Preliminary Results

To follow are results given for some preliminary survey simulations. The basic scanning algorithms used in these examples are intended primarily to show how the SEE environment can be used to compare the performance of various CAPS configurations using different NEO data sets. The first configuration examined will be a nonrealistic configuration in which the CAPS detectors are fixed inertially in space at the center of the target sphere (this location is the center of the Sun in the SEE space.) This case is intended to serve as a baseline to isolate the effects of the craft location and orbit motion on the effectiveness of the scan. The second configuration consists of two detectors in orbit about the Sun at a radius of 1 au. The third configuration consists of two detectors located on the Moon.

Case 1: Nonorbiting Detectors

In this case, two CAPS telescopes are fixed inertially at the center of the Sun. Each telescope contains a detector with a 1° square FOV. The stare-slew scan proceeds by slewing the detector to the target location and holding the detector fixed for the stare duration. The scan pattern moves the detector in an elevation sweep from the north celestial pole to the south celestial pole. In between each elevation sweep, an azimuth clock is performed to move the detector to a new celestial longitude. Figure 24 illustrates the scanning pattern. The view at left is looking down toward the south celestial pole and shows the detector FOV cones as black lines. The view at right illustrates the motion of the detector boresight as it performs an elevation sweep. The black circles are positions at which a stare occurs. The pattern also provides for a 5-percent overlap of the adjacent areas of the scan at the celestial equator. This scan requires ≈ 45 days to cover the entire celestial sphere. This simple scanning algorithm produces a large amount of undesirable overcoverage as the detector moves toward the poles (an alternative scanning algorithm with less overcoverage is also be examined).

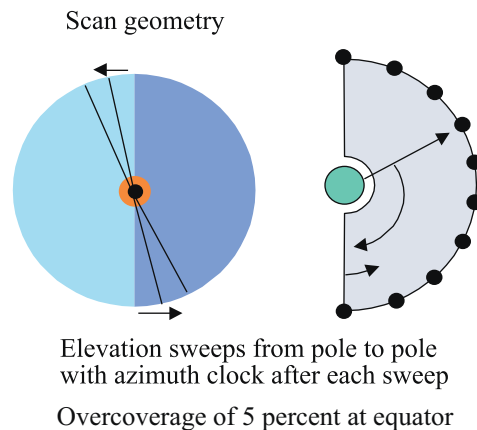


Figure 24. Case 1 initial scanning pattern.

The detector instrument is a telescope equipped with a charged-coupled device (CCD) array of pixel dimensions of 32000×32000 . Additional detector properties are as follows:

| | |
|------------------------------------|-------|
| Telescope optical diameter, m | 3.20 |
| Focal length/optical diameter, f/# | 5.20 |
| Resolution, arcsec/pixel | 0.10 |
| Quantum efficiency | 0.80 |
| Optical efficiency | 0.80 |
| Integration time, s, or dwell time | 90.00 |

The first NEO data set used in this case consisted of 8988 external returning comets (ERCs) with semimajor axes ranging from 33 to 10000 au and absolute magnitude ranging from 9.2 to 19. This data set was provided by Dr. William Bottke of Southwest Research Institute based on reference 2. These are simulated objects that were created using methods designed to produce realistic orbits based on known comets (ref. 3). None of the simulated objects is designed to necessarily impact the Earth. Each object was assigned an identical physical property as follows:

| | |
|-------------------|------|
| Diameter | 1 km |
| Albedo | 0.02 |
| Photometric slope | 0.15 |

The true anomaly of each object was set such that its heliocentric distance on the date that the scan begins was approximately 9 au (see fig. 25).

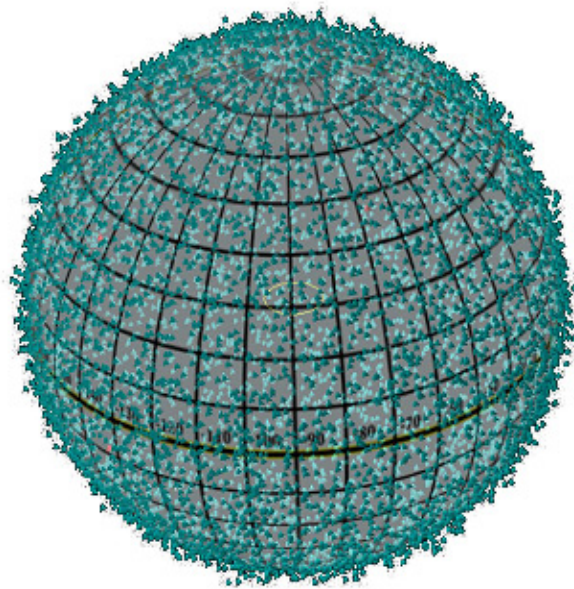


Figure 25. Visualization of ERC set at start of scan. The gridded sphere marks a heliocentric distance of 9 au. The density of the objects appears isotropic.

The summary report information generated by the SEE at the completion of this simulation is shown below:

Number of targets: 8988
Targets not scanned: 1
Targets with low per-pixel S/N (<6): 0

Total undetected targets: 1(0.0111259 %)

Signal-to-Noise Ratios
Highest: 11.1409 Lowest: 8.63558 Average: 10.3474

Per-Pixel Signal-to-Noise Ratios
Highest: 7.87783 Lowest: 6.10628 Average: 7.31668

Number of scopes: 2
Survey start date: 2000 01 01 00:00:00.000
Survey duration, days: 44.3345
Frame integration time, s: 90
Run time: 4 hr, 9 min, 35 s

Targets not scanned:
z_6059

Figure 22 includes the final coverage map. All areas of the target sphere have been covered by the scan. The high density of black outlines near the poles of map relative to a similar area at the equator indicates the severe overcoverage at high and low latitudes (see insets).

The “targets not scanned” category in the survey summary report refers to the number of objects never found in the FOV of any of the CAPS detectors. In this case, because our scan covered the entire celestial sphere, this could happen only if the NEO moved into a previously visited area of sky before the NEO’s original location had been visited. Review of the simulation graphics showed that object “z_6059” had indeed been located just west of the eastward-moving detector at the start of the simulation. By the end of the scanning period, the object had moved eastward into a previously covered area of sky. This object would have been observed within the first several hours if the scan had been allowed to repeat.

The “targets with low per-pixel S/N” category refers to objects that were scanned but would have gone undetected due to low per-pixel S/N ratio. In this example the cutoff value has been set to 6.0. The total S/N ratio for an object is a measure of the mean number of photons per unit time received by the detector. The per-pixel S/N ratio takes into account the number of pixels on the CCD over which this signal will be spread (a minimum of 1 pixel). An object with a higher angular rate relative to the detector will reduce the per-pixel S/N reading.

These preliminary results indicate that the detector parameters appear to be sufficient for observing 1-km ERCs with the given orbits and physical parameters. To examine the effect of faster moving NEOs, the case was repeated with a new object data set consisting of 8268 ERCs with true anomaly adjusted so

that the heliocentric distance was approximately 5 au. An excerpt from the summary report for this run is below:

Number of targets: 8268
Targets not scanned: 21
Targets with low S/N (<6): 0

Total undetected targets: 21(0.253991 %)

Signal-to-Noise Ratios
Highest: 40.8559 Lowest: 28.6865 Average: 35.3438

Per-Pixel Signal-to-Noise Ratios
Highest: 28.8895 Lowest: 14.5187 Average: 22.7721

In this case, 21 objects move in such a way as to avoid the scan pattern. Figure 26 shows a view of the objects looking toward the south celestial pole. These objects move in a clockwise direction, effectively following behind the detectors as they also move clockwise. The circle marks a radius of 1 au.

The next experiment utilizes a collection of 9001 simulated NEAs as the target set. These objects were also provided by Dr. William Bottke. The semimajor axis of these objects ranges from 0.4 to 7.4 au, and visual magnitudes range from 13.2 to 22. Figure 27 is a visualization of the object distribution, which shows a majority of low-inclination orbits.

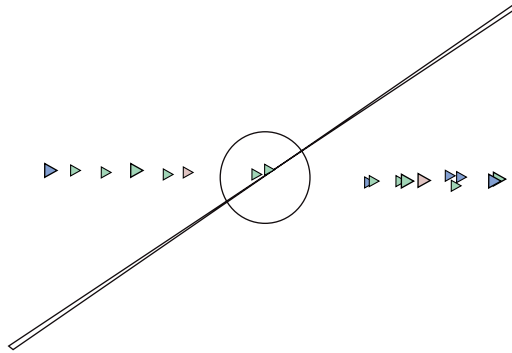


Figure 26. View of missed objects.

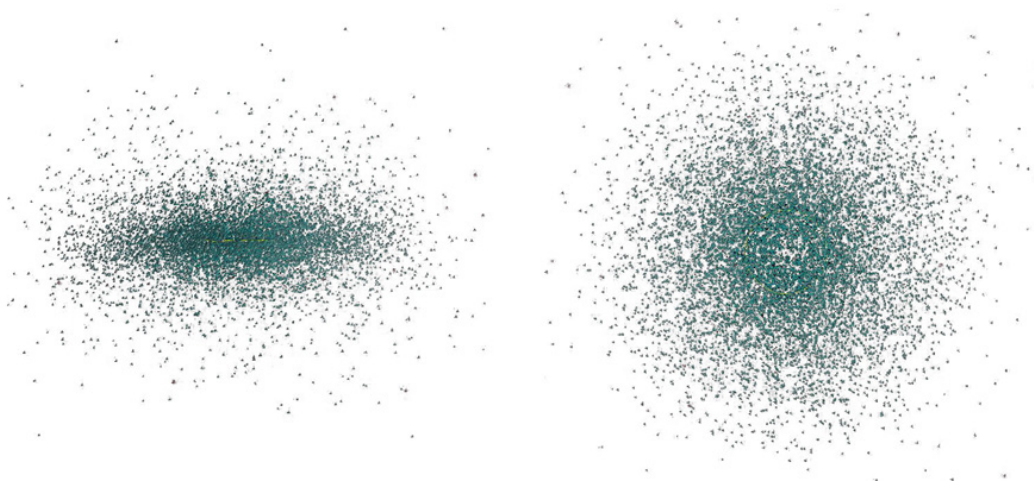


Figure 27. NEA distribution: View along ecliptic (left) and from the north celestial pole (right).

A repeat of the scanning simulation produced the following report:

Number of targets: 9001
Targets not scanned: 889
Targets with low per-pixel S/N (<6): 9
Total undetected targets: 898(9.97667 %)
Signal-to-Noise Ratios
Highest: 172158 Lowest: 5.28778 Average: 435.808
Per-Pixel Signal-to-Noise Ratios
Highest: 3402.03 Lowest: 3.73903 Average: 76.3751

A review of the visualization showed the majority of the nearly 900 unscanned objects were missed because their high velocities allowed them to pass between subsequent elevation sweeps in the scanning pattern. The nine objects with less than the minimum required per-pixel S/N ratio had absolute magnitudes greater than 19.

The last experiment in this case incorporated a new scanning strategy designed to reduce the over-coverage at areas near the poles. This strategy sweeps through arcs in azimuth with an elevation clock after every azimuth sweep. The scan starts at the north celestial pole and ends at the south celestial pole. The length of the azimuth arc is adjusted for the current elevation of the scan. The arc length is zero at the poles and largest at the celestial equator. The scan also incorporates a 5-percent coverage overlap at the equatorial azimuth sweep. A schematic of the scan strategy is shown in figure 28. The coverage map for this scan is shown in figure 29. Comparison of this map with figure 22 shows the reduced over-coverage of the poles for the azimuth-sweep strategy.

The improved scanning efficiency is reflected in the survey duration, which has been reduced from 44.3 days for full coverage for the elevation-sweep scan to 28.3 days for the azimuth-sweep scan. The results of a simulation using the improved scan strategy against the same NEA object data set are excerpted here from the summary report:

CAPS Survey Summary
Number of targets: 9001
Targets not scanned: 81
Targets with low per-pixel S/N (<6): 9
Total undetected targets: 90(0.999889 %)
Signal-to-Noise Ratios
Highest: 98052.7 Lowest: 5.29113 Average: 440.672
Per-Pixel Signal-to-Noise Ratios
Highest: 3093.17 Lowest: 3.74139 Average: 81.9013
Number of scopes: 2
Survey start date: 2000 01 01 00:00:00.000
Survey duration, days: 28.3514
Frame integration time, s: 90
Run time: 2 hr, 34 min, 30 s

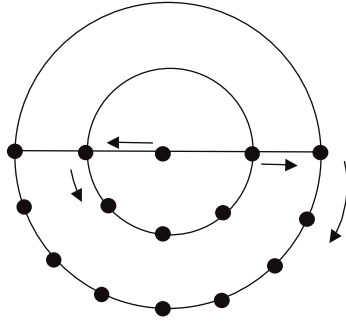


Figure 28. Scanning pattern using azimuth sweep. This view is looking down toward south pole of target sphere. The number of stare points in an azimuth sweep increases as elevation goes from pole to equator.

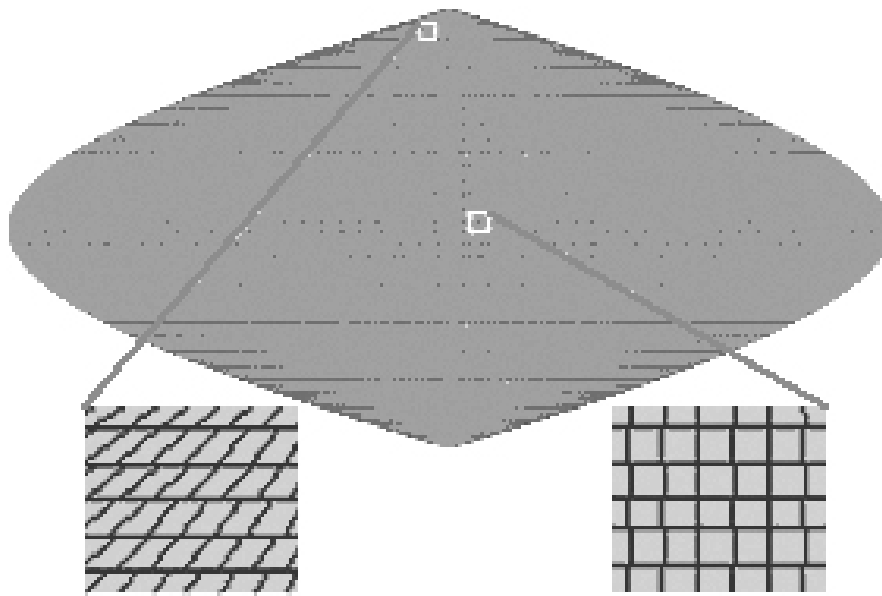


Figure 29. Survey map for azimuth-sweep scan pattern.

Also interesting is the substantially reduced number of unscanned objects (81 here versus 889 in the elevation-sweep strategy). Likely causes could be that the reduced time between subsequent passes of the azimuth sweep reduce the possibility of the NEO traveling far enough to evade detection, or that the azimuth sweeps are better aligned with the object trajectories. The nine low-signal objects are the objects with magnitudes greater than 19.

Case 2: Two-Location System

In this case, a detector is located on each of two crafts orbiting the Sun at 1 au. The scanning pattern is similar to the elevation-sweep method used at the start of case 1, but is adjusted for the fact that each detector in the two-location system needs to sweep over its local north and south poles in order to view the poles of the sun-centered target sphere. In figure 30, the left view shows the posigrade 1-au orbits of the two crafts, with the craft starting and ending positions as unfilled circles. The filled black circles indicate the positions of the crafts when the scan is at opposition. The right view shows that the elevation sweep spans more than 180° in order to cover the poles of the sun-centered target sphere.

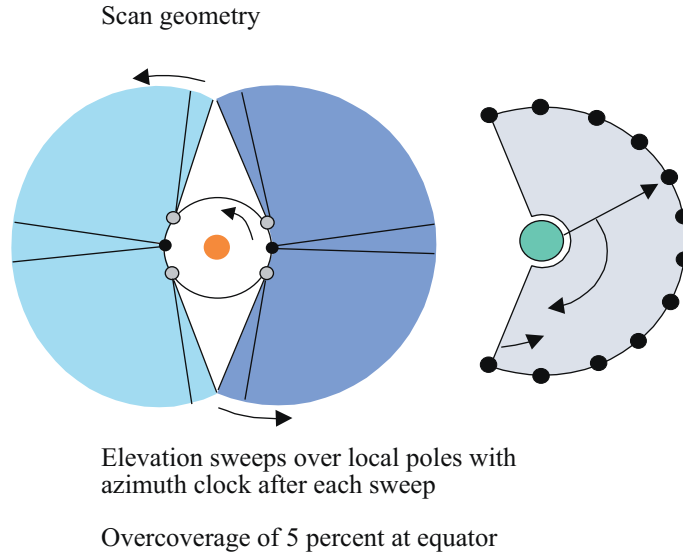


Figure 30. Two-location system scanning pattern.



Figure 31. Coverage map for two-location system, elevation-sweep scan, 9-au target sphere.

The coverage map for this pattern is shown in figure 31. Note that because the detector locations are offset from the target sphere origin, the radius of the target sphere will affect the amount of coverage registered by the map. While this effect can be mitigated by selecting a “celestial” sphere with infinite radius, the coverage of such a sphere is not necessarily a desirable metric for the CAPS system. Because the NEOs of interest are within approximately 9 AU, the desirable metric will be one that indicates the volume of space covered by the detectors in this region. To examine the coverage at other heliocentric distances, the simulation can be programmed to produce multiple maps, although with increasing expense in simulation time and memory usage. Because of these difficulties, selecting a method for measuring the combined coverage of a two-location system in the space near the detectors will be an important design consideration for further CAPS survey simulations.

The NEOs used in this run were the ERCs in case 1 whose heliocentric distances were approximately 9 au at the beginning of the scan; therefore, a single 9-au sun-centered target sphere was used. The scan

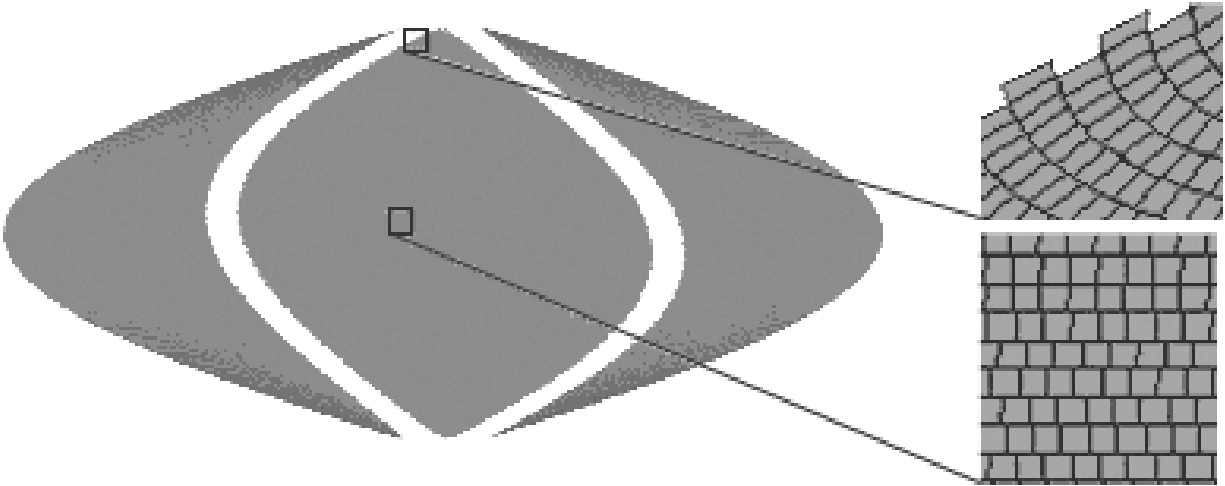


Figure 32. Coverage map for two-location system, 180° elevation span.

was terminated when the elevation sweeps had covered all longitudes along the equator. The wedge-shaped gaps in the map are an effect of the off-opposition scanning geometry, where the north-to-south motion of the detector was not corrected to maintain alignment with the lines of longitude on the target sphere. Subsequent repeats of the scan will tend to fill in these gaps as the motion of the craft causes the scan opposition point to move.

In this case, 204 objects were not scanned due to the gaps in coverage. No objects had less than the minimum S/N ratio of 6.0. The scan took 51 days to complete the coverage at the equator.

This simulation was also run using the 5-au ERCs and a subset of NEA objects used in case 1 (the reduced NEA set contains only objects with absolute magnitude greater than 19.1). Again it was seen that the faster moving objects caused an increasing number of missed sightings. Of the 8268 ERCs at 5 au, 461 were unscanned. Of the 2383 NEAS, 892 were not scanned and two objects had low per-pixel S/N measurements.

The azimuth-sweep scanning strategy used to reduce overcoverage at the celestial poles was also attempted in this case. Figures 17 and 15 show the coverage results for two versions of the azimuth-sweep strategy. In figure 32, the azimuth-sweep span is 180° of the elevation on a sphere centered at the detector. The 1-au distance from the detector location to the 9-au sun-centered target sphere origin causes the gaps in the target sphere coverage. Figure 33 includes the results of adjusting the scan to cover 200° of elevation at the local sphere in order to get better coverage of the 9-au sun-centered target sphere. The duration of the scans shown in figures 32 and 33 were 28 and 31 days, respectively.

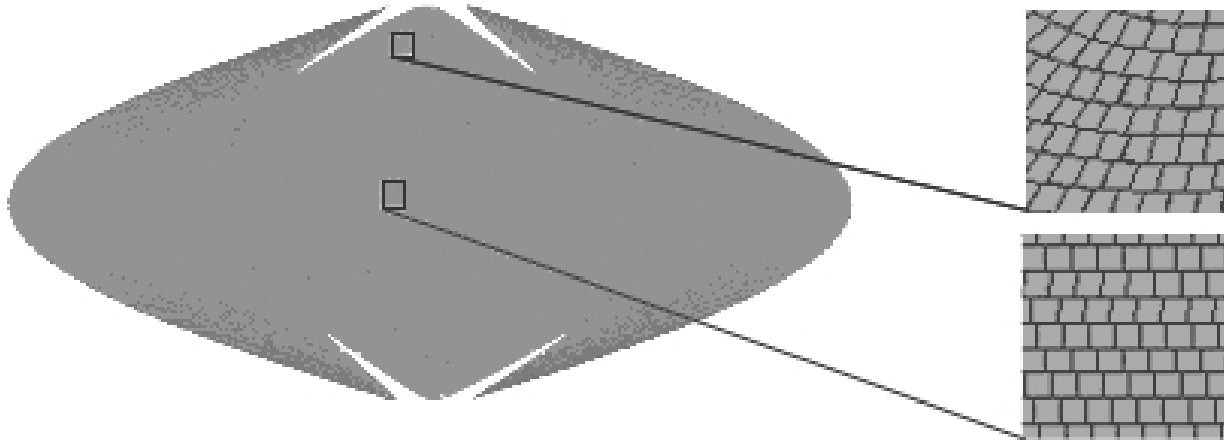


Figure 33. Coverage map for two-location system, 200° elevation span.

Case 3: Two Detectors on the Surface of the Moon

The geometry of this CAPS survey configuration is shown in figure 34. The view at left shows the view from the Moon's equator of the elevation sweeps. The view at right shows the visualization graphics of the scaled-up Moon bases and the detector view frusta. The two detectors are located on the Moon surface at 75° north and south latitude. The north detector is at 90° east longitude, and the south detector is at 90° west longitude. Each moon-based detector is performing an elevation sweep designed to cover the northern or southern hemisphere of a 9-au target sphere centered at the Sun. The rotation of the Moon itself is used to change the azimuth of the detector, so no azimuth clock is performed. The scan was terminated after 28.5 days. The coverage map (fig. 35) illustrates that the azimuth rate introduced by the Moon's rotation is too large to allow full coverage at the equator. To improve coverage at the equator, the elevation-sweep scan pattern must reduce coverage at the poles or use a smaller dwell time or a larger view frustum.

The coverage results for an alternative configuration with the detectors located directly on the lunar poles, each using an azimuth-sweep scan to cover half of the sun-centered 9-au target sphere, are given in figure 36. A full 360° azimuth sweep is performed at each elevation. After a complete azimuth sweep, an elevation clock of 0.95° is performed and a new azimuth sweep is started. The duration of the survey was 28.5 days. Overall coverage appears improved over the elevation-sweep scan. Small horizontal strips of missed coverage are caused by the rotation of the Moon. Revision of the scanning program to account for this effect could provide 100-percent coverage with little additional scanning time. The effect of occlusion of the detectors by the Earth will, however, substantially affect the real coverage results near the lower scan elevations.

The scan shown in figure 36 was performed on the collection of 2383 NEAs used in case 2. Sixty of the objects were unscanned and two were missed due to low signal. This result is consistent with the trend that patterns sweeping generally along lines of latitude (azimuth sweep) rather than lines of longitude (elevation sweep) have been more effective in reducing the number of missed NEAs.

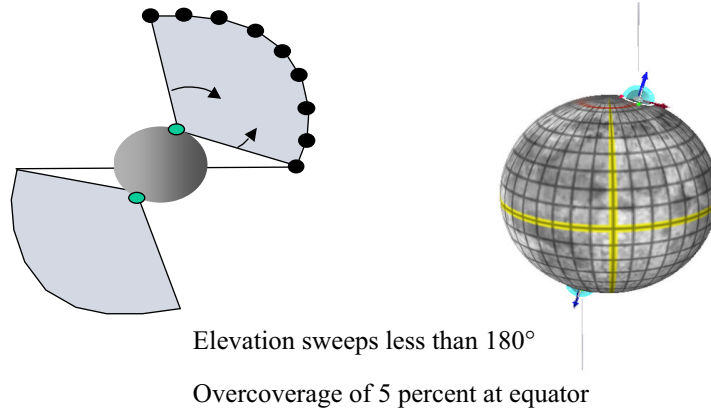


Figure 34. Moon-based system scanning pattern.

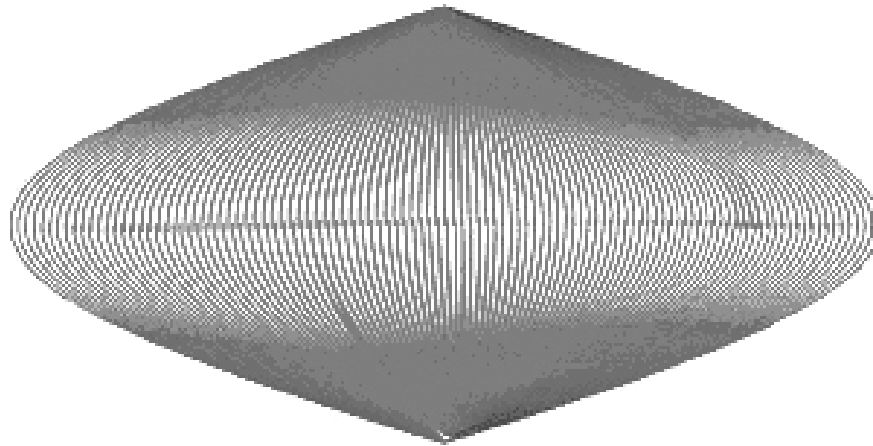


Figure 35. Coverage map for moon-based detectors with elevation-sweep scan.

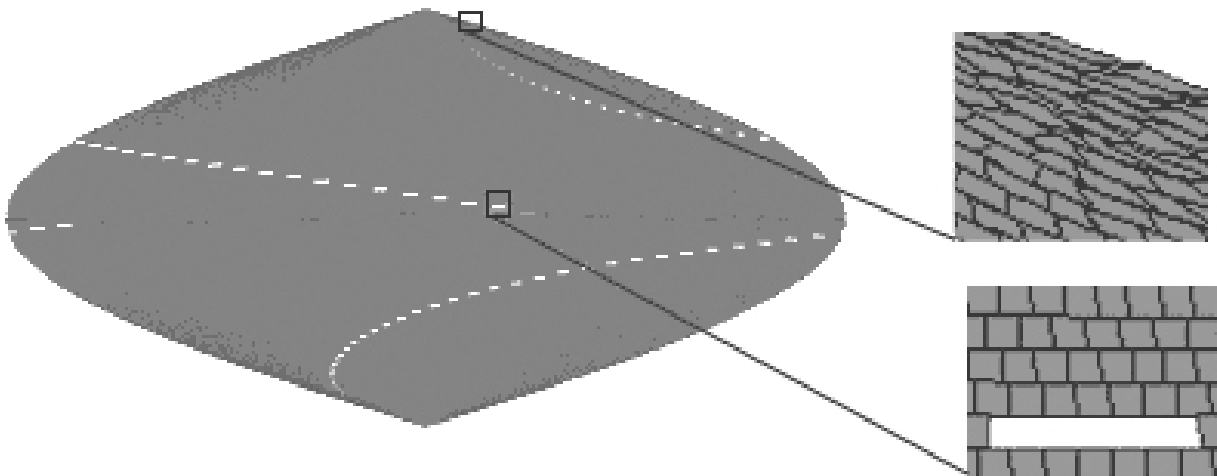


Figure 36. Coverage map for moon-based detectors with azimuth-sweep scan.

Concluding Remarks

The beginnings of an integrated Comet/Asteroid Protection System (CAPS) simulation and visualization tool have been constructed in the Synergistic Engineering Environment (SEE) application. The availability of interactive three-dimensional views of the scene geometry assists in evaluating the effectiveness of proposed detection systems and in improving their designs. The preliminary examination of several proposed survey configurations against simulated near-Earth object (NEO) data sets showed the ability of the SEE to compare the efficiency of different scanning algorithms. The problem of designing an effective scanning algorithm was shown to be closely tied to the problem of establishing a valid survey coverage metric when the system contains more than one detector location. It was demonstrated that a scan pattern achieving full coverage of a given area on a target sphere can miss substantial numbers of fast moving objects due to the objects' motion between subsequent passes of a sweeping-style scan. To counter this effect, a successful scanning pattern should consider the geometry of the object paths.

The future development of the SEE for CAPS would benefit from addition of the following features:

- Sophisticated scanning algorithms that allow multiple craft to work together to provide full coverage of the target volume with minimum overcoverage.
- Modeling of survey detector frustum occlusion by solid objects or light sources.
- Volume rendering of the coverage map showing overcoverage at all distances between a minimum and maximum radii of the target coverage volume.
- Near-Earth object-creation routine to automatically create object trajectories that will impact the Earth at a user specified date.
- Further integration with the Coverage Analysis Tool separate from the SEE used in the orbit determination and orbit modification sections of this report.

References

1. Tegmark, M.: An Icosahedron-Based Method for Pixelizing the Celestial Sphere. *Appl. J. Lett.*, vol. 470, 2001, p. 81.
2. Wiegert, P.; and Tremaine, S.: The Evolution of Long-Period Comets. *Icarus*, vol. 137, issue 1, Jan. 1999, pp. 84–121.
3. Levison, H. F.; Morbidelli, A.; Dones, L.; Jedicke, R.; Wiegert, P. A.; and Bottke, W. F.: The Mass Disruption of Oort Cloud Comets. *Science*, vol. 296, June 21, 2002, pp. 2212–2215.